

University of Nebraska - Lincoln

DigitalCommons@University of Nebraska - Lincoln

---

Biological Systems Engineering: Papers and Publications

Biological Systems Engineering

---

2010

## Net Radiation Dynamics: Performance of 20 Daily Net Radiation Models as Related to Model Structure and Intricacy in Two Climates

Suat Irmak

University of Nebraska-Lincoln, suat.irmak@unl.edu

Denis Mutiibwa

University of Nebraska-Lincoln, mutiibwa2000@yahoo.com

José O. Payero

University of Nebraska-Lincoln, jpayero@clmson.edu

Follow this and additional works at: <https://digitalcommons.unl.edu/biosysengfacpub>



Part of the [Biological Engineering Commons](#)

---

Irmak, Suat; Mutiibwa, Denis; and Payero, José O., "Net Radiation Dynamics: Performance of 20 Daily Net Radiation Models as Related to Model Structure and Intricacy in Two Climates" (2010). *Biological Systems Engineering: Papers and Publications*. 235.  
<https://digitalcommons.unl.edu/biosysengfacpub/235>

This Article is brought to you for free and open access by the Biological Systems Engineering at DigitalCommons@University of Nebraska - Lincoln. It has been accepted for inclusion in Biological Systems Engineering: Papers and Publications by an authorized administrator of DigitalCommons@University of Nebraska - Lincoln.

# NET RADIATION DYNAMICS: PERFORMANCE OF 20 DAILY NET RADIATION MODELS AS RELATED TO MODEL STRUCTURE AND INTRICACY IN TWO CLIMATES

S. Irmak, D. Mutiibwa, J. O. Payero

**ABSTRACT.** We compared daily net radiation ( $R_n$ ) estimates from 19 methods with the ASCE-EWRI  $R_n$  estimates in two climates: Clay Center, Nebraska (sub-humid) and Davis, California (semi-arid) for the calendar year. The performances of all 20 methods, including the ASCE-EWRI  $R_n$  method, were then evaluated against  $R_n$  data measured over a non-stressed maize canopy during two growing seasons in 2005 and 2006 at Clay Center. Methods differ in terms of inputs, structure, and equation intricacy. Most methods differ in estimating the cloudiness factor, emissivity ( $\epsilon$ ), and calculating net longwave radiation ( $R_{nl}$ ). All methods use albedo ( $\alpha$ ) of 0.23 for a reference grass/alfalfa surface. When comparing the performance of all 20  $R_n$  methods with measured  $R_n$ , we hypothesized that the  $\alpha$  values for grass/alfalfa and non-stressed maize canopy were similar enough to only cause minor differences in  $R_n$  and grass- and alfalfa-reference evapotranspiration ( $ET_o$  and  $ET_r$ ) estimates. The measured seasonal average  $\alpha$  for the maize canopy was 0.19 in both years. Using  $\alpha = 0.19$  instead of  $\alpha = 0.23$  resulted in 6% overestimation of  $R_n$ . Using  $\alpha = 0.19$  instead of  $\alpha = 0.23$  for  $ET_o$  and  $ET_r$  estimations, the 6% difference in  $R_n$  translated to only 4% and 3% differences in  $ET_o$  and  $ET_r$ , respectively, supporting the validity of our hypothesis. Most methods had good correlations with the ASCE-EWRI  $R_n$  ( $r^2 > 0.95$ ). The root mean square difference (RMSD) was less than  $2 \text{ MJ m}^{-2} \text{ d}^{-1}$  between 12 methods and the ASCE-EWRI  $R_n$  at Clay Center and between 14 methods and the ASCE-EWRI  $R_n$  at Davis. The performance of some methods showed variations between the two climates. In general,  $r^2$  values were higher for the semi-arid climate than for the sub-humid climate. Methods that use dynamic  $\epsilon$  as a function of mean air temperature performed better in both climates than those that calculate  $\epsilon$  using actual vapor pressure. The ASCE-EWRI-estimated  $R_n$  values had one of the best agreements with the measured  $R_n$  ( $r^2 = 0.93$ ,  $\text{RMSD} = 1.44 \text{ MJ m}^{-2} \text{ d}^{-1}$ ), and estimates were within 7% of the measured  $R_n$ . The  $R_n$  estimates from six methods, including the ASCE-EWRI, were not significantly different from measured  $R_n$ . Most methods underestimated measured  $R_n$  by 6% to 23%. Some of the differences between measured and estimated  $R_n$  were attributed to the poor estimation of  $R_{nl}$ . We conducted sensitivity analyses to evaluate the effect of  $R_{nl}$  on  $R_n$ ,  $ET_o$ , and  $ET_r$ . The  $R_{nl}$  effect on  $R_n$  was linear and strong, but its effect on  $ET_o$  and  $ET_r$  was subsidiary. Results suggest that the  $R_n$  data measured over green vegetation (e.g., irrigated maize canopy) can be an alternative  $R_n$  data source for  $ET$  estimations when measured  $R_n$  data over the reference surface are not available. In the absence of measured  $R_n$ , another alternative would be using one of the  $R_n$  models that we analyzed when all the input variables are not available to solve the ASCE-EWRI  $R_n$  equation. Our results can be used to provide practical information on which method to select based on data availability for reliable estimates of daily  $R_n$  in climates similar to Clay Center and Davis.

**Keywords.** Albedo, Alfalfa-reference evapotranspiration, Evapotranspiration, Grass-reference evapotranspiration, Maize, Net radiation, Penman-Monteith.

**N**et radiation ( $R_n$ ) is the difference between total downwelling and upwelling radiation fluxes and is a measure of the radiant energy exchange at the earth's surface. It is one of the primary driving

forces in the surface energy balance, including latent heat (evapotranspiration,  $ET$ ), and other biological and biophysical processes. Most  $ET$  equations and micrometeorological and surface-atmosphere energy exchange studies require  $R_n$ . The accuracy of the estimations of  $ET$  and other dynamics of energy exchange mechanisms depends on accurate quantification of this variable. Limitations in measured  $R_n$  data have been a persistent problem in studies involving land surface-atmosphere interactions, hydrologic modeling, micrometeorology, and water resources management in agro-ecological landscapes. Although the number of automated weather stations that monitor major climate variables has been increasing in the last two decades, the number of weather stations that have net radiometers is still limited because direct measurement of  $R_n$  is an expensive task and involves vigorous maintenance for the net radiometers. Thus, estimation of  $R_n$  from air temperature, total incoming shortwave solar radiation ( $R_s$ ), and other climatic variables remains the dominant approach in most parts of the U.S. and around the world. In the U.S., the ratio between stations measuring  $R_n$

Submitted for review in August 2009 as manuscript number SW 8136; approved for publication by the Soil & Water Division of ASABE in June 2010.

The mention of trade names or commercial products is solely for the information of the reader and does not constitute an endorsement or recommendation for use by the University of Nebraska-Lincoln or the authors.

The authors are **Suat Irmak, ASABE Member Engineer**, Associate Professor, and **Denis Mutiibwa, ASABE Member Engineer**, Graduate Research Assistant, Department of Biological Systems Engineering, University of Nebraska-Lincoln, Lincoln, Nebraska; **José O. Payero**, Research Scientist, Irrigated Farming Systems, Department of Primary Industries and Fisheries, Toowoomba, Australia. **Corresponding author:** Suat Irmak, Department of Biological Systems Engineering, University of Nebraska-Lincoln, 241 L.W. Chase Hall, Lincoln, NE 68583; phone: 402-472-4865; fax: 402-472-6338; e-mail: sirmak2@unl.edu.

and those observing only primary climatic variables such as  $R_s$ , air temperature, relative humidity, and rainfall is approximately 1:100 (Thornton and Running, 1999). For example, the High Plains Regional Climate Center (Hubbard, 1992) operates approximately 70 weather stations throughout Nebraska and another approximately 120 automated weather stations in neighboring states, none of which monitor  $R_n$ . Furthermore, the density of weather stations that observe air temperature and  $R_s$  to estimate  $R_n$  is not nearly enough to make spatial estimates of  $R_n$  for determining spatial distribution of surface energy balance components in agro-ecological settings.

Adding to the issues involved with an insufficient density of stations that observe  $R_n$ , net radiometers are one of the most delicate sensors used in agro-meteorological stations. Extensive maintenance, cost, calibration, and other challenges, such as the variability between different brands of sensors and inaccuracies of the measurements when the sensor is moistened by rain, irrigation water, or dew formation, led to the development of methods to estimate  $R_n$  from surface characteristics and climatic variables. An additional difficulty is the requirement that  $R_n$  be measured over irrigated and well-maintained reference surfaces when used in grass- or alfalfa-reference  $ET$  ( $ET_o$  and  $ET_r$ , respectively) calculations. This is particularly difficult in arid and semi-arid regions, where maintaining a large number of irrigated and well-maintained reference surface sites of large enough size (i.e.,  $\geq 4$  ha) for automated weather station networks is a formidable and very expensive task. One alternative approach would be to use  $R_n$  measured over other vegetation surfaces for  $ET$  estimations or to use microclimatic variables measured over other green vegetation surfaces to estimate  $R_n$ . In recent years, in addition to the automated weather stations, surface energy flux measurement systems, such as the Bowen ratio energy balance system (BREBS; Bowen, 1926; Tanner, 1960; Denmead and McIlroy, 1970; Fuchs and Tanner, 1970); eddy covariance system (ECS; Swinbank, 1951; Deacon and Swinbank, 1958; Tanner, 1960; Dyer, 1961; Webb et al., 1980; Aubinet et al., 2001, Finnigan et al., 2003); and surface renewal (SR; Paw et al., 1995; Snyder et al., 1996, 2008) are being used over various vegetation surfaces to monitor surface energy balance components, including  $R_n$ , for research and other purposes. Thus, the  $R_n$  and microclimatic measurements from these systems could be another potential source of data for  $R_n$  for  $ET$  estimations of other surfaces. In addition, in many cases, these surface energy balance systems are the only source of data to quantify  $R_n$  and/or  $ET$  for other surfaces due to absence of automated reference weather stations in the area for which the  $R_n$  and  $ET$  estimations are needed.

Numerous methods have been developed to estimate  $R_n$ . The models differ in the intricacy of their calibration structure and in their use of climatic parameters, variables, and coefficients. The primary differences among them revolve around the procedures used to compute clear-sky solar radiation, net outgoing longwave radiation, atmospheric emissivity, and actual vapor pressure of the air. A developed and tested robust set of equations has been compiled and published by the ASCE Environmental and Water Resources Institute (ASCE-EWRI, 2005), and these procedures have been suggested as the standardized procedures to estimate  $R_n$  (this method is referred to the ASCE-EWRI  $R_n$  method in our study). The ASCE-EWRI  $R_n$  calculation procedures have also been recommended for estimating  $ET_o$  and  $ET_r$  using

standardized ASCE-Penman-Monteith equation (ASCE-EWRI PM) (ASCE-EWRI, 2005).

Although the ASCE-EWRI approach for predicting  $R_n$  is widely used in the U.S. and around the world, studies that compare these procedures with other empirical procedures and with measured  $R_n$  data are limited. Most  $R_n$  methods, including the ASCE-EWRI, require measured  $R_s$  data. Use of measured  $R_s$  to compute  $R_n$  reduces the computational intensity and minimizes the error from calculating  $R_s$  using an estimation of relative sunshine duration ( $n/N$ , the ratio of actual measured bright sunshine hours and maximum possible sunshine hours). Relative sunshine duration is the ratio that indicates the cloudiness of the atmosphere, which was first proposed by Angström (1924) to estimate  $R_s$ . The net outgoing shortwave radiation ( $R_{so}$ ) required for computing net longwave radiation ( $R_{nl}$ ) can be estimated using a number of methods. The ASCE-EWRI (2005) recommends four methods to compute  $R_{so}$  depending on the calibration constants, air turbidity, and elevation. However, the ASCE-EWRI does not present an assessment of how different  $R_{nl}$  computations might impact  $R_n$ ,  $ET_r$ , and  $ET_o$ . In addition, the ASCE-EWRI  $R_n$  procedure requires the input parameters of  $R_s$ , maximum and minimum air temperature ( $T_{max}$  and  $T_{min}$ ), dew point temperature ( $T_{dew}$ ), and maximum and minimum relative humidity ( $RH_{max}$  and  $RH_{min}$ ). Given the limitations in availability and quality of climatic data, especially in developing countries, there is a need to evaluate the performance of different  $R_n$  calculation procedures relative to the ASCE-EWRI  $R_n$  method and measured  $R_n$  data. Although the ASCE-EWRI approach represents a standardized way of computing  $R_n$ , in many cases the availability and quality of input parameters dictate which  $R_n$  method can be used.

We compared daily  $R_n$  estimates from 19 methods to ASCE-EWRI  $R_n$  estimates in two climates: a transition zone between semi-humid and semi-arid climates at Clay Center, Nebraska, and a Mediterranean-type semi-arid climate at Davis, California. The performance of all 20  $R_n$  methods, including the ASCE-EWRI  $R_n$  method, were then evaluated using measured  $R_n$  over a non-stressed maize canopy for Clay Center for two growing seasons in 2005 and 2006. In comparing the measured  $R_n$  over the maize canopy with the  $R_n$  estimated based on a grass-reference surface, our hypothesis was that the albedo ( $\alpha$ ) values of maize and grass and alfalfa ( $\alpha = 0.23$ ) were similar and that minor differences in  $\alpha$  (e.g., up to 20%) would not impact the  $R_n$  and  $ET$  estimations significantly. We tested this hypothesis by quantifying the impact of using different  $\alpha$  values on  $R_n$ ,  $ET_o$ , and  $ET_r$ . We also discuss the model performance in relation to the model structure and complexity.

## MATERIALS AND METHODS

### CLIMATE DATA AND STATISTICAL ANALYSES

The climate data measured at two locations were used: Clay Center, Nebraska (40° 34' N, 98° 8' W, 552 m above mean sea level, MSL) and Davis, California (38° 32' 09" N, 121° 46' 32" W, 18 m above MSL). Measured daily weather data for a 20-year period (1 January 1983 to 31 December 2004) at Clay Center and for a 14-year period (1 January 1990 to 31 December 2004) at Davis were used. Clay Center datasets were obtained from the High Plains Regional Climate Center (HPRCC; www.hprcc.unl.edu). Davis datasets were

obtained from the California Department of Water Resources, California Irrigation Management Information System (CIMIS) (Snyder and Pruitt, 1992) ([www.cimis.water.ca.gov](http://www.cimis.water.ca.gov)). The type of instrumentation and placement heights for each site were reported by Irmak et al. (2006). Weather variables measured at these stations included wind speed at 2 m height ( $u_2$ ),  $T_{max}$ ,  $T_{min}$ ,  $RH_{max}$ ,  $RH_{min}$ , rainfall, and  $R_s$ . The ASCE-EWRI  $R_n$  calculation procedures were used as the reference method to predict daily  $R_n$ . The  $R_n$  comparisons between ASCE-EWRI  $R_n$  vs. all other 19 methods were made on a daily basis for the two locations for the calendar year. The performances of all 20  $R_n$  methods, including the ASCE-EWRI  $R_n$  method, were then compared with the measured data for Clay Center from 1 June to 30 September in 2005 and from 1 June to 20 September in 2006. The coefficient of determination ( $r^2$ ), slope, and root mean square difference (RMSD) were computed to quantify over- and underpredictions and performance of each  $R_n$  method. A two-tailed t-test (for two-sample for means) was performed to identify whether  $R_n$  estimates from the 20 methods were significantly different from the measured  $R_n$  values at Clay Center at the 5% significance level. The null hypothesis was that the method-estimated and measured  $R_n$  values came from the same population and that the hypothesized (null hypothesis) mean difference between estimated and measured  $R_n$  values was zero. Further analyses were done to quantify the differences between method-estimated  $R_{nl}$  and ASCE-EWRI-estimated  $R_{nl}$ . We quantified the differences between the method-estimated  $R_{nl}$ , including the ASCE-EWRI  $R_{nl}$ , with the measured  $R_{nl}$  for Clay Center. Sensitivity analyses were conducted to quantify the sensitivity of  $R_n$ ,  $ET_o$ , and  $ET_r$  to  $R_{nl}$ , and also to evaluate the sensitivity of  $R_n$ ,  $ET_o$ , and  $ET_r$  to  $\alpha$ . Since the estimated  $R_n$  data from the 20 methods tested and the ASCE-EWRI estimated  $R_n$  data are time series data on a daily time step, there is a probability that autocorrelation (AC) exists between the method-estimated and ASCE-EWRI-estimated  $R_n$  data. More importantly, autocorrelation in the residuals of regression obtained from regression analysis of method-estimated  $R_n$  versus ASCE-EWRI  $R_n$  or in the paired differences of  $R_n$  estimates and measured  $R_n$  values may affect the estimation of regression parameter estimates (slope and intercept) and model RMSD, and/or the significance of paired t-tests, respectively. In order to investigate and address potential autocorrelation, regression models were constructed using PROC AUTOREG (SAS/STAT v. 9.2, SAS Institute, Inc., Cary, N.C.), and the residuals of the  $R_n$  data were tested for each method. The Durbin-Watson test was used to check for the first-order autocorrelation of the residuals.

#### GENERAL FIELD EXPERIMENTAL PROCEDURES

Field experiments for measurements of  $R_n$  were conducted at the University of Nebraska-Lincoln, South Central Agricultural Laboratory (SCAL) near Clay Center, Nebraska, in 2005 and 2006. SCAL is located approximately 160 km west of Lincoln in the south central part of the state. The  $R_n$  measurements were made over a non-stressed maize (*Zea mays* L.) canopy. We hypothesized that the maize had a similar  $\alpha$  value as the grass- or alfalfa-reference surface and that using  $R_n$  measured above the maize canopy would not significantly influence the  $ET$  estimations when  $R_n$  was estimated with the 19 methods as compared with the measured values.

Maize (hybrid Pioneer 33B51 with a comparative relative maturity of 113 days) was planted at 0.76 m row spacing with a seeding rate of approximately 73,000 seeds  $ha^{-1}$  and a planting depth of 0.05 m in an east-west row direction. In 2005, maize was planted on 22 April, emerged on 12 May, matured on 7 September, and was harvested on 17 October. In 2006, maize was planted on 12 May, emerged on 20 May, matured on 13 September, and was harvested on 5 October. The hybrid had 2,730 growing degree units to black layer with 113 to 114 days to maturity and was a non-prolific hybrid that had flex ear characteristics (ear length changes in response to environmental characteristics). The maximum maize height was measured as 2.50 m on 20 July 2005 and 31 July 2006. The experimental field (13.8 ha) was irrigated with subsurface drip irrigation system. Detailed descriptions of the additional experimental site and soil and plant management practices were reported by Irmak et al. (2008) and Irmak and Mutibwa (2008). Drip laterals were spaced every 1.5 m (every other plant row) in the middle of the furrow and were installed approximately 0.40 m below the soil surface. Irrigations were applied three times a week to meet the plant water requirement. A total of 225 and 172 mm of irrigation water was applied during the 2005 and 2006 growing seasons, respectively. A total of 283 and 330 mm of rainfall occurred during the growing season in 2005 and 2006, respectively.

#### FIELD MEASUREMENT OF RADIATION ENVELOPES

Net radiation and other microclimatic variables in the maize field were measured using a deluxe version of a Bowen ratio energy balance system (BREBS; Radiation and Energy Balance Systems, REBS, Inc., Bellevue, Wash.). The BREBS and data used in this study are part of the Nebraska Water and Energy Flux Measurement, Modeling and Research Network (NEBFLUX) (Irmak, 2010) that operates ten deluxe version of BREBS and one eddy covariance system over various vegetation surfaces ranging from irrigated and rainfed grasslands, tilled and untilled, and irrigated and rainfed croplands to Phragmites (*Phragmites australis*)-dominated cottonwood (*Populus deltoides* var. *occidentalis*) and willow stand (*Willow salix*) plant communities. Detailed description of the microclimate measurements, including latent heat flux, sensible heat flux, soil heat flux, net radiation, and other microclimatic variables (vapor pressure, air temperature, relative humidity, wind speed and direction, incoming and outgoing shortwave radiation, albedo, and soil temperature) were presented by Irmak (2010) and only a brief description of some of the primary measurements using the BREBS will be presented here.  $R_n$  was measured using a REBS Q\*7.1 net radiometer that was installed approximately 4.5 m above the canopy. The radiometer is sensitive to wavelengths from 0.25 to 60  $\mu m$ . It is attached to a 4 m long metal arm to extend the radiometer away from the tripod (horizontally to the plant canopy) so that only the  $R_n$  at the canopy/soil surface is measured and the reflection of heat and radiation from any other instruments and equipment (i.e., solar panel, etc.) installed on the tripod is eliminated. The net radiometer had two type-E chromel-constantan differential thermocouple junctions that are installed to monitor temperature differences between the core and upper and lower windshields (domes). The net radiometer was supplied with constant air blown through a desiccant tube to keep the air inside the dome dry so that formation of condensation inside the dome was eliminated. Incoming and outgoing shortwave and long-

wave radiation were measured simultaneously using a REBS model THRDS7.1 double-sided total hemispherical radiometer that was sensitive to wavelengths from 0.25 to 60  $\mu\text{m}$ . The surface  $\alpha$  was calculated as the ratio of outgoing shortwave to incoming shortwave radiation. All variables were sampled at 30 s intervals and then averaged and recorded every hour using a model CR10X datalogger and AM416 relay multiplexer (Campbell Scientific, Logan, Utah). The BREBS maintenance on a weekly basis included cleaning the thermocouples, servicing the radiometers by cleaning or replacing the domes, checking/replacing the desiccant tubes, and making sure that the net and solar radiometers were properly leveled.

#### ASCE-EWRI $R_n$ CALCULATION PROCEDURES

The ASCE-EWRI  $R_n$  calculation procedures as outlined in ASCE-EWRI (2005) are as follows:

$$R_n = R_{ns} \downarrow - R_{nl} \uparrow \quad (1)$$

where

- $R_n$  = net radiation ( $\text{MJ m}^{-2} \text{d}^{-1}$ )
- $R_{ns}$  = incoming net shortwave radiation ( $\text{MJ m}^{-2} \text{d}^{-1}$ )
- $R_{nl}$  = outgoing net longwave radiation ( $\text{MJ m}^{-2} \text{d}^{-1}$ ).

The  $R_{ns}$  is a result of the balance between incoming and reflected solar radiation as a function of  $\alpha$ :

$$R_{ns} = (1 - \alpha)R_s \downarrow \quad (2)$$

where

- $\alpha$  = albedo or canopy reflection coefficient (fixed at 0.23 for a green vegetation surface)
- $R_s$  = total incoming shortwave solar radiation ( $\text{MJ m}^{-2} \text{d}^{-1}$ ).

The rate of  $R_{nl}$  is proportional to the fourth power of the absolute temperature of the surface:

$$R_{nl} = \sigma \left[ \frac{T_{max,K}^4 + T_{min,K}^4}{2} \right] (0.34 - 0.14\sqrt{e_a}) \times \left( 1.35 \frac{R_s}{R_{so}} - 0.35 \right) \quad (3)$$

where

- $\sigma$  = Stefan-Boltzmann constant ( $4.903 \times 10^{-9} \text{ MJ K}^{-4} \text{ m}^{-2} \text{ d}^{-1}$ )
- $T_{max,K}$  = daily maximum absolute air temperature ( $\text{K} = ^\circ\text{C} + 273.16$ )
- $T_{min,K}$  = daily minimum absolute air temperature ( $\text{K} = ^\circ\text{C} + 273.16$ )
- $e_a$  = actual vapor pressure of the air (kPa)
- $R_{so}$  = calculated clear-sky solar radiation ( $\text{MJ m}^{-2} \text{d}^{-1}$ ).

The actual vapor pressure is calculated as:

$$e_a = 0.6108 \exp \left[ \frac{17.27T_{dew}}{T_{dew} + 237.3} \right] \quad (4)$$

where  $T_{dew}$  is the dew point temperature ( $^\circ\text{C}$ ). Depending on the availability of data,  $e_a$  can be calculated using  $RH$  and/or  $T_{min}$ .

Doorenbos and Pruitt (1977) developed an equation to calculate daily values of  $R_{so}$  as a function of station elevation ( $z$ , m) and extraterrestrial radiation ( $Ra$ ,  $\text{MJ m}^{-2} \text{d}^{-1}$ ) as:

$$R_{so} = (0.75 + 2 \times 10^{-5} z) Ra \downarrow \quad (5)$$

Daily  $Ra$  ( $\text{MJ m}^{-2} \text{d}^{-1}$ ) can be calculated as a function of day of the year, solar constant and declination, and latitude:

$$Ra = \frac{1440}{\pi} G_{sc} d_r \times [\omega_s \sin(\varphi) \sin(\delta) + \cos(\varphi) \cos(\delta) \sin(\omega_s)] \quad (6)$$

where

- $G_{sc}$  = solar constant ( $0.0820 \text{ MJ m}^{-2} \text{min}^{-1}$ )
- $d_r$  = inverse relative distance from earth to sun
- $\omega_s$  = sunset hour angle (rad)
- $\varphi$  = latitude (rad)
- $\delta$  = solar declination (rad)

$$\delta = 0.4093 \sin \left( \frac{2\pi(284 + J)}{365} \right) \quad (7)$$

where  $J$  is the day of the year (1 to 366)

$$d_r = 1 + 0.033 \cos \left( \frac{2\pi J}{365} \right) \quad (8)$$

$$\omega_s = \arccos(\psi) \quad (9)$$

$$\psi = \tan(\varphi) \tan(\delta) \quad (10)$$

#### NET RADIATION CALCULATION PROCEDURE FOR 19 OTHER $R_n$ METHODS

The following section provides brief background information and describes the general procedures and common equations used in the different  $R_n$  methods for the calculation of various parameters and variables. Descriptions of the equation structure, coefficients, and variables used for each  $R_n$  method are provided later in this article. Dew point temperature, used in equation 4 to compute  $e_a$ , was not measured at either study location and was computed using the following equation (Murray, 1967):

$$T_{dew(i)} = \frac{237.3}{\left[ 1 / \left( \frac{\ln RH_i}{17.27} \right) + \left( \frac{T_i}{237.3} + T_i \right) \right]^{-1}} \quad (11)$$

where  $RH_i$  is the mean relative humidity (%) for period  $i$ , and  $T_i$  is the mean temperature ( $(T_{max} + T_{min})/2$ ,  $^\circ\text{C}$ ) for period  $i$ .

Net shortwave radiation ( $R_{ns}$ ) is the balance of incoming and reflected solar radiation.  $R_s$  can be calculated using Angström's formula, as recommended by Doorenbos and Pruitt (1977):

$$R_s = \left( 0.25 + 0.5 \frac{n}{N} \right) Ra \quad (12)$$

where  $n/N$  is the ratio of actual measured bright sunshine hours and maximum possible sunshine hours. Besides the

temperature and humidity,  $R_{nl}$  is influenced by cloudiness and by the difference between temperatures of the surface and the air. Jensen et al. (1990) presented a general formula for calculating  $R_{nl}$ :

$$R_{nl} = f\varepsilon\sigma T^4 \quad (13)$$

where  $\sigma$  is the Stefan-Boltzmann constant ( $4.895 \times 10^{-9}$  MJ  $m^{-2} d^{-1} K^{-4}$ ),  $T$  is the average air temperature,  $f$  is a factor to adjust for cloud cover, and  $\varepsilon$  is the atmospheric emissivity. Wright and Jensen et al. (1972) proposed the following equation for  $f$ :

$$f = a \frac{R_s}{R_{so}} + b \quad (14)$$

and Brunt (1932) developed an empirical equation for atmospheric  $\varepsilon$ :

$$\varepsilon = a_1 + b_1 \sqrt{e_a} \quad (15)$$

where  $a = 1.35$ ,  $b = -0.34$ ,  $a_1 = 0.35$ , and  $b_1 = -0.14$ ;  $e_a$  is calculated using equation 4.

Wright (1982) presented an approach for dynamic values of  $a$ ,  $b$ , and  $a_1$ :

for  $R_s/R_{so} > 0.7$ :  $a = 1.126$  and  $b = -0.07$

for  $R_s/R_{so} \leq 0.7$ :  $a = 1.017$  and  $b = -0.06$ .

$$a_1 = 0.26 + 0.1 \exp\left\{-\left(0.0154(30m + N - 207)\right)^2\right\} \quad (16)$$

where  $m$  is the month, and  $N$  is the day of year

Another equation, which requires only mean air temperature to estimate  $\varepsilon$ , was presented by Idso et al. (1969) and Idso and Jackson (1969):

$$\varepsilon = -0.02 + 0.261 \exp[-7.77 \times 10^{-4} (273 - T)^2] \quad (17)$$

To compute  $f$  to adjust for cloud cover, one can obtain estimated values of  $R_{so}$  by plotting observed  $R_s$  values to obtain an envelope curve through the maximum radiation values. Allen et al. (1998) presented two procedures to calculate  $R_{so}$ . If the calibrated values of  $a_s$  and  $b_s$  are available, equation 18 is recommended:

$$R_{so} = (a_s + b_s) R_a \quad (18)$$

Doorenbos and Pruitt (1977) recommended using 0.25 and 0.50 for  $a_s$  and  $b_s$ , respectively. For areas with high turbidity or when the sun angle is less than  $50^\circ$ , Allen et al. (1998) recommended equation 19 to calculate  $R_{so}$ . This equation is applicable when the calibrated values are not available only for station elevations less than 6,000 m having low air turbidity:

$$R_{so} = R_a \exp\left(\frac{-0.0018P}{K_t \sin \phi}\right) \quad (19)$$

where  $P$  is the atmospheric pressure (kPa),  $K_t$  is the turbidity coefficient ( $0 < K_t \leq 1.0$ ; 1.0 for clean air; and 0.1 for extremely turbid, dusty, or polluted air), and  $\phi$  is the sun angle above the horizon (rad). For daily calculations,  $\phi$  can be determined as:

$$\sin \phi_{24} =$$

$$\sin \left[ 0.85 + 0.3\phi \sin \left( \frac{2\pi}{365} J - 1.39 \right) - 0.42\phi^2 \right] \quad (20)$$

where  $\phi_{24}$  is average sun angle during the daylight period, weighted according to  $R_a$ .

Allen (1997) suggested that the estimation for  $R_{so}$  can be improved by considering the effect of water vapor on shortwave absorption, as incorporated into equation 21:

$$R_{so} = (K_B + K_D) R_a \quad (21)$$

where  $K_B$  is the clearness index for direct beam radiation, and  $K_D$  is the corresponding index for diffuse beam radiation and is computed as:

$$K_B = 0.98 \exp \left[ \frac{-0.00146P}{K_t \sin \phi} - 0.091 \left( \frac{W}{\sin \phi} \right)^{0.25} \right] \quad (22)$$

$$W = 0.14e_a P + 2.1 \quad (23)$$

where  $W$  is the precipitable water vapor in the atmosphere (mm), and all other parameters have been previously defined.  $K_D$  is estimated from  $K_B$  as:

$$K_D = 0.35 - 0.33K_B \text{ for } K_B \geq 0.15 \quad (24)$$

$$K_D = 0.18 + 0.82K_B \text{ for } K_B < 0.15 \quad (25)$$

Using a cosine function and data from NOAA (1977-1980) for the western U.S., Heermann et al. (1985) derived an empirical equation to describe daily  $R_{so}$  (MJ  $m^{-2} d^{-1}$ ) for the calendar year:

$$R_{so} = A' + B' \cos \left[ \frac{2\pi J}{365 - C'} \right] \quad (26)$$

where  $A' = 31.55 - 0.273L + 0.0008A$  and  $B' = -0.299 + 0.268L + 0.0004A$ , where  $L$  = latitude ( $^\circ$ ) and  $A$  = altitude (m).  $C'$  is a phase constant theoretically set to 2.92 and corresponds to the longest day of the year (21 June), and the cosine function is for values in radians. Jensen et al. (1990) developed a linear equation correlating  $R_n$  with  $R_s$ :

$$R_n = a_3 R_s + b_3 \quad (27)$$

where the regression coefficients,  $a_3 = 0.61$  and  $b_3 = -1.0$ , were obtained by averaging data from 14 locations worldwide. With the objective of developing alternative equations to reduce the input and computational intensity for FAO Irrigation and Drainage Paper No. 56 (Allen et al., 1998)  $R_n$  calculation procedures, Irmak et al. (2003) derived two equations to predict daily  $R_n$  using minimum climatological data. The first equation (the measured  $R_s$ -based equation) requires  $T_{max}$ ,  $T_{min}$ , measured  $R_s$ , and  $d_r$  as input parameters:

$$R_n = (-0.054T_{max}) + (0.111T_{min}) + (0.462R_{s(measured)}) + (-49.243d_r) + 50.831 \quad (28)$$

where the units of  $T_{max}$ ,  $T_{min}$ , and  $R_s$  (measured) are  $^\circ C$ ,  $^\circ C$ , and MJ  $m^{-2} d^{-1}$ , respectively. The second equation (the predicted  $R_s$ -based equation) requires  $T_{max}$ ,  $T_{min}$ ,  $RH_{mean}$ , and predicted  $R_s$ :

$$R_n = (-0.09T_{max}) + (0.203T_{min}) - (0.101RH_{min}) + (0.687R_{s(predicted)}) + 3.97 \quad (29)$$

In equation 29,  $R_s$  is predicted using the Hargreaves and Samani (1982) and Samani (2000) equation:

$$R_s = (KT)(R_a)(TD)^{0.5} \quad (30)$$

where  $TD = T_{max} - T_{min}$  ( $^{\circ}C$ ), and  $KT$  is an empirical coefficient. Allen (1997) suggested using  $KT = 0.17(P/P_o)^{0.5}$  for interior regions and  $KT = 0.2(P/P_o)^{0.5}$  for coastal regions (elevations <1500 m), where  $P$  is mean monthly atmospheric pressure (kPa), and  $P_o$  is mean monthly atmospheric pressure at sea level (kPa).

Using equation 2,  $R_{ns}$  was estimated from measured  $R_s$  for Clay Center and Davis. To account for the effect of cloud cover and  $\epsilon$  of the maize canopy,  $R_{nl}$  was estimated using equation 13 through 15.  $R_{nl}$  was also measured at Clay Center using the BREBS. Five different equations (eqs. 5, 18, 19, 21, and 26) were used to estimate  $R_{so}$ .  $R_{so}$  was also measured using the BREBS at Clay Center. Parameters  $a$  and  $b$  in equation 14, to adjust for cloud cover, were used both as constants and variables in the different  $R_n$  methods. The value of  $\epsilon$  was computed using two equations (eqs. 15 and 17). Parameters  $a_1$  and  $b_1$  in equation 15 were also used as constants and variables by some of the  $R_n$  methods. The following section outlines the variables and constants used by each of the 19 methods to compute  $R_n$ . The structure of each  $R_n$  method, its input requirements, and its calculation steps are presented in table 1. All methods, except methods 15, 16, and 17, use the same form of equation 1 and calculate  $R_n$  as a difference between  $R_{ns}$  and  $R_{nl}$ . All methods, except methods 15, 16, and 17, use equation 2 to compute  $R_{ns}$ . Methods 15, 16, and 17 estimate  $R_n$  directly from  $R_s$  (i.e.,  $R_{ns}$  is not calculated). Three of the 19  $R_n$  methods use estimated

$R_s$ . Methods 17, 18, and 19 use either equation 12 or equation 30 to estimate  $R_s$  using the  $n/N$  ratio and  $Ra$  as constants.

The following example illustrates how the 19  $R_n$  methods were used to compute  $R_n$  as a function of different parameters and constants. As shown in table 1, method 1 uses measured  $R_s$ . The  $R_{so}$  for method 1 was calculated using equation 18. The  $R_{ns}$  was calculated as a function of  $\alpha$  and  $R_s$  using equation 2. The  $R_{nl}$  was calculated using equation 13. Parameters  $a$  and  $b$  in the calculation of factor  $f$  were taken as constants ( $a = 1.35$ ;  $b = -0.34$ ). The net atmospheric emissivity ( $\epsilon$ ) was calculated using equation 17 as a function of air temperature. Equation 17 does not use parameters  $a_1$  and  $b_1$ . Finally, the daily  $R_n$  value for method 1 was calculated using the difference between  $R_{ns}$  and  $R_{nl}$  (eq. 1). Similar examples can be followed to identify which methods use which equations, constants, variables, or parameters to compute  $R_n$ . In table 1, the ASCE-EWRI  $R_n$  method is not listed because this method uses equations 1 through 10.

#### CALCULATION OF GRASS- AND ALFALFA- REFERENCE EVAPOTRANSPIRATION

The impact of different  $\alpha$  values on  $ET_o$  and  $ET_r$  was determined by solving the ASCE-EWRI PM equation with two  $\alpha$  values. The ASCE-EWRI PM equation is intended to simplify and clarify the application of the method and associated equations for computing aerodynamic and bulk surface resistance ( $r_a$  and  $r_s$ , respectively). Equations were combined into a single expression for grass- and alfalfa-reference surfaces and for a daily time step by varying coefficients. The equation as presented by ASCE-EWRI (2005) is:

$$ET_{ref} = \frac{0.408\Delta(R_n - G) + \gamma \frac{C_n}{T + 273} u_2 (e_s - e_a)}{[\Delta + \gamma(1 + C_d u_2)]} \quad (31)$$

Table 1. Structure of the methods used to compute  $R_n$  as a function of variables, constants, and equations.[a]

$R_n$ Method	$R_{ns}$ (eq. 2) $R_s$	$R_{nl}$ (eq. 13)		
		$f$ (from eq. 14)		$\epsilon$
		$R_{so}$	$a$ and $b$	$a_1$ and $b_1$
1	Measured	Eq. 18	$a = 1.35$ ; $b = -0.34$	Eq. 17 --
2	Measured	Eq. 5	$a = 1.35$ ; $b = -0.34$	Eq. 15 $a_1$ variable; $b_1 = 0.139$
3	Measured	Eq. 19	$a = 1.35$ ; $b = -0.34$	Eq. 17 --
4	Measured	Eq. 21	Variable	Eq. 17 --
5	Measured	Eq. 26	Variable	Eq. 15 $a_1$ variable; $b_1 = 0.139$
6	Measured	Eq. 18	Variable	Eq. 15 $a_1 = 0.35$ ; $b_1 = -0.14$
7	Measured	--	--	Eq. 17 --
8	Measured	--	--	Eq. 15 $a_1$ variable; $b_1 = 0.139$
9	Measured	--	--	Eq. 15 $a_1 = 0.35$ ; $b_1 = -0.14$
10	Measured	Eq. 5	Variable	Eq. 17 --
11	Measured	Eq. 26	$a = 1.35$ ; $b = -0.34$	Eq. 17 --
12	Measured	Eq. 18	Variable	Eq. 15 $a_1$ variable; $b_1 = 0.139$
13	Measured	Eq. 5	Variable	Eq. 15 $a_1 = 0.35$ ; $b_1 = -0.14$
14	Measured	Eq. 21	$a = 1.35$ ; $b = -0.34$	Eq. 15 $a_1$ variable; $b_1 = 0.139$
15 (eq. 27) <sup>[b]</sup>	Measured	--	--	-- --
16 (eq. 28) <sup>[b]</sup>	Measured	--	--	-- --
17 (eq. 29) <sup>[b]</sup>	Eq. 30	--	--	-- --
18	Eq. 12	Eq. 19	$a = 1.35$ ; $b = -0.34$	Eq. 15 $a_1 = 0.35$ ; $b_1 = -0.14$
19	Eq. 12	Eq. 19	Variable	Eq. 15 $a_1$ variable; $b_1 = 0.139$

[a] All methods, except methods 15, 16, and 17, use the same form of equation 1 and calculate  $R_n$  as the difference between  $R_{ns}$  and  $R_{nl}$ . The ASCE-EWRI  $R_n$  method uses equations 1 through 10 to calculate  $R_n$  and is not included in the table as one of the 19  $R_n$  methods.

[b]  $R_{ns}$  is not calculated for equations 15, 16, and 17.

where

- $ET_{ref}$  = standardized grass- or alfalfa-reference  $ET$  (mm d<sup>-1</sup>)
- $\Delta$  = slope of saturation vapor pressure versus air temperature curve (kPa °C<sup>-1</sup>)
- $R_n$  = net radiation at the surface (MJ m<sup>-2</sup> d<sup>-1</sup>)
- $G$  = heat flux density at the soil surface (assumed zero for daily time step)
- $T$  = mean daily air temperature (°C)
- $u_2$  = mean daily or hourly wind speed at 2 m height (m s<sup>-1</sup>)
- $e_s$  = saturation vapor pressure (kPa)
- $e_a$  = actual vapor pressure (kPa)
- $e_s - e_a$  = vapor pressure deficit (kPa)
- $\gamma$  = psychrometric constant (kPa °C<sup>-1</sup>)
- $C_n$  and  $C_d$  = numerator and denominator constants, respectively, that change with reference surface and calculation time step
- 0.408 = coefficient (m<sup>2</sup> mm MJ<sup>-1</sup>).

The values of  $C_n$  and  $C_d$  for grass- and alfalfa-reference surface for daily time steps are presented in table 2. All  $ET_{ref}$  calculations were done on a daily basis. Measured  $RH_{max}$ ,  $RH_{min}$ ,  $T_{max}$ , and  $T_{min}$  values were used to calculate  $e_a$  and  $e_s$ . A value of  $1.013 \times 10^{-3}$  MJ kg<sup>-1</sup> °C<sup>-1</sup>, which represents an average value of specific heat ( $c_p$ ) at constant temperature, was used in the calculations;  $\gamma$  was computed as a function of atmospheric pressure ( $P$ ),  $c_p$ , and ratio of molecular weight of water vapor to dry air (0.622) for each study site, and  $P$  was calculated as a function of station elevation,  $z$  (m) as:

**Table 2. Values of  $C_n$  and  $C_d$  for grass and alfalfa reference for daily and hourly time steps as reported by ASCE-EWRI (2005).<sup>[a]</sup>**

Time Step	Grass Reference ( $ET_o$ )		Alfalfa Reference ( $ET_r$ )	
	$C_n$	$C_d$	$C_n$	$C_d$
Daily	900	0.34	1600	0.38
Hourly during daytime	37	0.24	66	0.25
Hourly during nighttime	37	0.96	66	1.7

<sup>[a]</sup>  $C_n$  is in units of °C mm s<sup>3</sup> Mg<sup>-1</sup> d<sup>-1</sup> for 24 h time step and °C mm s<sup>3</sup> Mg<sup>-1</sup> h<sup>-1</sup> for hourly time step.  $C_d$  is in units of s m<sup>-1</sup> for 24 h and hourly time step.

$$P = 101.3 \left( \frac{293 - 0.0065z}{293} \right)^{5.26} \quad (32)$$

## RESULTS AND DISCUSSION

### MEASURED RADIATION ENVELOPES

Measured radiation envelopes ( $R_s$ ,  $R_n$ , and  $R_{nl}$ ) for the 2005 and 2006 seasons for Clay Center are presented in figures 1a and 1b, respectively.  $R_s$  was the largest and  $R_{nl}$  was the smallest component of the radiation envelope. In general,  $R_s$  and  $R_n$  were largest in late July and decreased toward the end of the season.  $R_{nl}$  was smallest early in the season due to reduced reflection of radiation from the soil surface during partial canopy cover.  $R_{nl}$  increased toward the midseason as the canopy developed full closure, increasing reflection.  $R_{nl}$  ranged between 1.3 MJ m<sup>-2</sup> d<sup>-1</sup> in early June and about 5 MJ

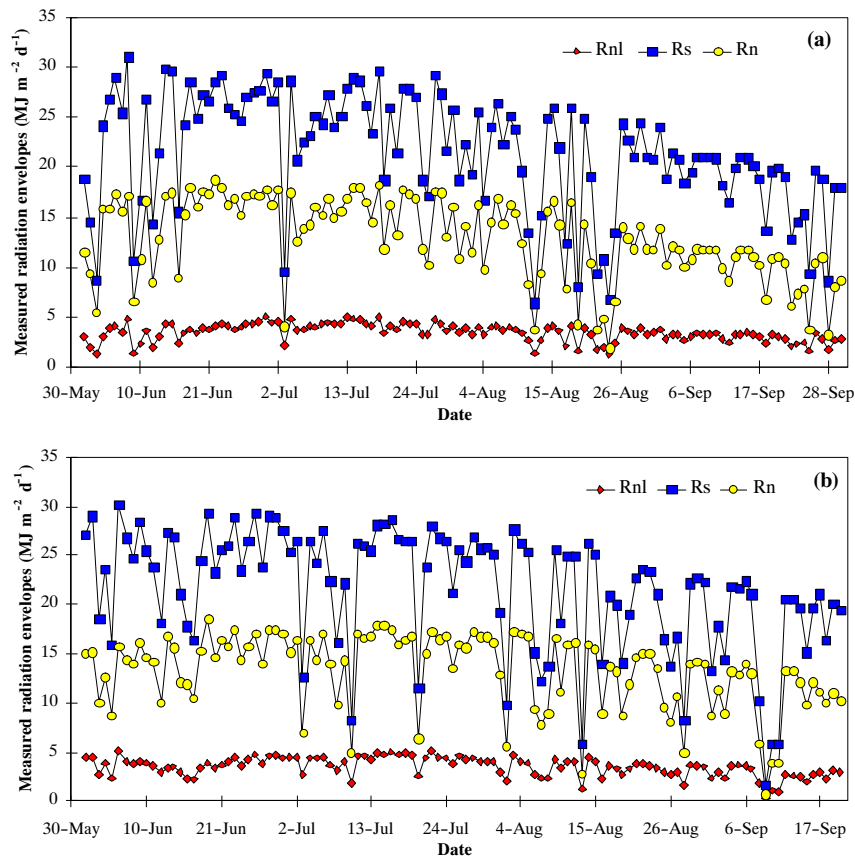


**Figure 1. Seasonal distribution of measured daily radiation envelopes, including incoming shortwave radiation ( $R_s$ ), net radiation ( $R_n$ ), and outgoing net longwave radiation ( $R_{nl}$ ) for the (a) 2005 and (b) 2006 seasons.**

$\text{m}^{-2} \text{d}^{-1}$  in mid-to-late July in both years. The largest day-to-day variability was in  $R_s$ , as a function of cloud cover, and  $R_s$  ranged from 6.4 to 31.1  $\text{MJ m}^{-2} \text{d}^{-1}$  in 2005 and from 1.7 to 30.7  $\text{MJ m}^{-2} \text{d}^{-1}$  in 2006, with seasonal averages of 12.8 and 13.3  $\text{MJ m}^{-2} \text{d}^{-1}$  for 2005 and 2006, respectively. Overall, the maximum values of the radiation components were greater in 2005 due to less cloud cover, but the seasonal average values were greater in 2006. When the two years of data are pooled, on a seasonal average basis,  $R_n$  was about 60% of  $R_s$ .  $R_{nl}$  represented a small portion of  $R_s$  due to the interception of  $R_s$  at the surface and diffusion within the canopy.  $R_{nl}$  was about 16% of  $R_s$  in both years.  $R_n$  started to decrease from middle to late August in both seasons. During this time, leaf aging and senescence started reducing the  $\alpha$  and  $R_n$  of the canopy due to increase in  $R_{ns}$  and due to a reduced amount of  $R_s$  toward the end of the season.

#### MEASURED ALBEDO AND TESTING THE HYPOTHESIS OF THE ALBEDO SIMILARITY BETWEEN MAIZE AND GRASS/ALFALFA CANOPIES

We present the seasonal distribution of daily  $\alpha$  data measured over maize canopy in figure 2 for 2005 and 2006. Daily  $\alpha$  values were obtained from hourly ratios of outgoing shortwave to incoming shortwave radiation. Hourly  $\alpha$  values were obtained for a given day when  $R_s > 0$  and averaged for the day. In 2005, the  $\alpha$  increased gradually from approximately 0.15 early in the season to a maximum of around 0.23 in mid-season and gradually decreased to a range of 0.16 to 0.18 at the end of September during physiological maturity. The minimum  $\alpha$  occurred on 4 June as 0.14, and the maximum occurred on 3 July, 26 July, and 12 August as 0.23. We observed similar trends in 2006. The seasonal average  $\alpha$  was the same (0.19) in both years, which is 17% less than the commonly used value of 0.23 for grass and alfalfa surface. Our results are comparable with those reported by other researchers. Monteith (1959) made extensive measurements of surface  $\alpha$  for various vegetation and reported  $\alpha$  values for grass as 0.24 to 0.26, alfalfa as 0.16 to 0.22, and for 0.60 to 2.1 m tall maize canopy as 0.16 to 0.17. Monteith and Unsworth (1990) reported an average  $\alpha$  of 0.24 for grass and 0.18 to 0.22 for maize canopy. Brutsaert (1982) grouped grass and other short green plants (maize, alfalfa, potatoes, beets) under the same category and reported an  $\alpha$  range of 0.15 to 0.25 for these surfaces. Sellers (1965) and Oke (1978) grouped most of the green agronomical plants into one group

and suggested an  $\alpha$  range of 0.10 to 0.25. Thus, it appears that  $\alpha$  values reported in the literature for maize, grass, and alfalfa are very similar and vary in a narrow range.

Penman (1956) and Penman et al. (1967) suggested that the changes in plant color have very little influence on  $\alpha$  and that the differences in  $ET$  caused by differences in  $\alpha$  for agronomical vegetation are quite modest. Most agronomical vegetation surfaces have similar color. Grass and maize are both C4 grass-type plants and have similar plant physiological functions. Thus, one would expect the  $\alpha$  values to be similar for both surfaces (Penman, 1956). It was an important step for us to demonstrate whether this assumption holds when comparing the measured  $R_n$  data over the maize canopy and estimated  $R_n$  data using grass-reference  $\alpha$  (0.23) from all 20  $R_n$  methods to quantify how much potential difference between the two  $R_n$  values are due to measurement of  $R_n$  over maize rather than grass canopy. We tested our hypothesis of  $\alpha$  values being similar for maize and grass canopies and that slight differences would not cause significant differences in  $R_n$ ,  $ET_o$ , and  $ET_r$  calculations in two ways. First, we estimated  $R_n$  using 2005 data for Clay Center from measured climatic variables for  $\alpha = 0.23$  and  $\alpha = 0.19$  (fig. 3). The  $\alpha$  value of 0.19 is the seasonal average value that we measured over the maize canopy in both seasons. The two  $R_n$  estimations were within 6%, with  $R_n$  estimated using  $\alpha = 0.19$  having the larger estimates. The two  $R_n$  estimations had a small RMSD (0.89  $\text{MJ m}^{-2} \text{d}^{-1}$ ) and high  $r^2$  (1.0). The magnitude of  $R_n$  estimated using  $\alpha = 0.19$  is greater than that of  $R_n$  estimated using  $\alpha = 0.23$ , using  $\alpha = 0.23$ , and the difference between the two  $R_n$  values increases at larger  $R_n$  values to a maximum difference of 6%. Based on the paired sample t-test (two-samples for means), the two  $R_n$  values were not significantly different at the 5% significance level ( $p > 0.05$ , table 3), supporting our hypothesis.

We quantified the impact of using  $\alpha = 0.19$  instead of  $\alpha = 0.23$  in calculation of  $R_n$  on  $ET_o$  and  $ET_r$  estimates using the ASCE-EWRI PM equation (eq. 31) for the 2005 data. Both daily  $ET_o$  and  $ET_r$  estimated using  $\alpha = 0.23$  and  $\alpha = 0.19$  exhibited the same seasonal trend with almost identical magnitude throughout the season (fig. 4). Regression analyses (fig. 5) showed that the  $ET_o$  values calculated using  $\alpha = 0.23$  and  $\alpha = 0.19$  were within 4% (fig. 5a) with a low RMSD of 0.22  $\text{mm d}^{-1}$ , and the  $ET_r$  values were within 3% (fig. 5b) with a similar RMSD (0.21  $\text{mm d}^{-1}$ ). Thus, while using  $\alpha = 0.19$  instead of  $\alpha = 0.23$  resulted in 6% difference

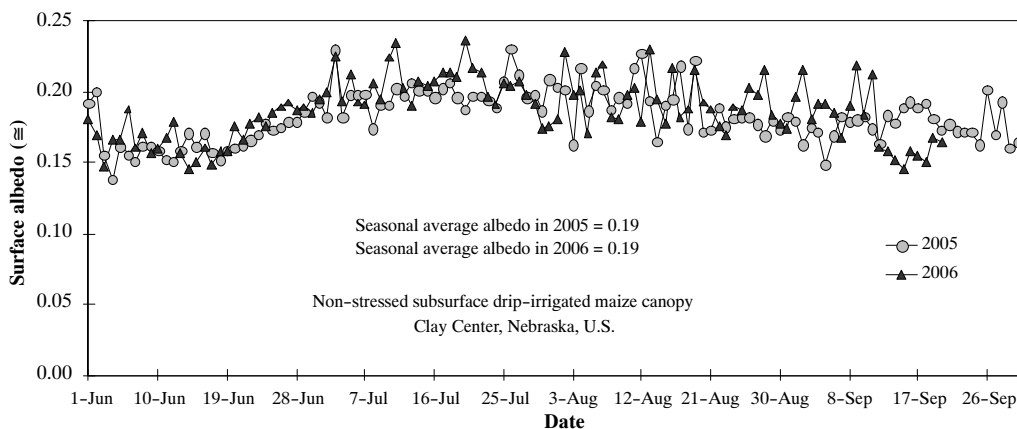


Figure 2. Seasonal distribution of daily surface albedo ( $\alpha$ ) over a non-stressed maize canopy for 2005 and 2006 growing seasons.

in  $R_n$ , this difference was translated to only 4% and 3% difference in  $ET_o$  and  $ET_r$ , respectively. The statistical analyses showed that the  $ET_o$  and  $ET_r$  values calculated using  $\alpha = 0.23$  and  $\alpha = 0.19$  were not significantly different ( $p > 0.05$ , paired sample t-test, table 3). The analyses of  $R_n$ ,  $ET_o$ , and  $ET_r$  calculated using  $\alpha = 0.23$  vs.  $\alpha = 0.19$  indicated that our hypothesis that the  $\alpha$  values for the maize and grass canopy are similar and that even some quantity of difference (17%) between the two would not cause a significant difference when computing  $R_n$ ,  $ET_o$ , and  $ET_r$  is valid. Thus, we conclude that the performance of all 20 methods, which use  $\alpha = 0.23$ , can be statistically compared with the  $R_n$  data measured over maize canopy.

The statistical analyses results for autocorrelation for the residuals of regression between method-estimated  $R_n$  and the ASCE-EWRI-estimated  $R_n$  data and associated intercept and slopes are presented in table 4. Table 4 also includes the regress r-squared (RRS coeff.) between the residuals ASCE-EWRI  $R_n$  and method-estimated  $R_n$ , which ranges from 0 to 1. The outputs of the first-order Durbin-Watson test (DW) for significance are also included. The results are significant with positive autocorrelation ( $p < 0.05$ ) for methods 4, 7, 8, 9, 10, 13, 15, and 18 at Clay Center, whereas seven methods (4, 7, 8, 9, 10, 15, and 16) had significant autocorrelation at Davis.

#### COMPARISONS OF ESTIMATED DAILY $R_n$ FROM 19 METHODS WITH ASCE-EWRI-ESTIMATED $R_n$

Figures 6 and 7 present the regression analysis comparing the performance of the 19  $R_n$  methods with the ASCE-EWRI  $R_n$  for Clay Center and Davis, respectively. The relationships

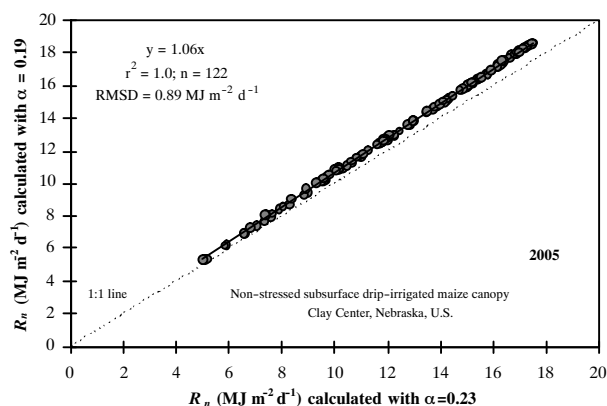


Figure 3. Relationship between net radiation ( $R_n$ ) calculated using surface albedo ( $\alpha$ ) of 0.23 vs.  $R_n$  calculated using  $\alpha = 0.19$  for a non-stressed maize canopy.

are presented in figures rather than in a tabular format to better visualize the data distribution in the entire range of  $R_n$  values and to better visualize the over- and underestimations in different  $R_n$  ranges. All methods, except for methods 15, 16, and 17, differ in estimating the cloudiness factor and  $\epsilon$  for calculating  $R_{nl}$ . Overall, the majority of the methods had a good correlation with the ASCE-EWRI  $R_n$  ( $r^2 > 0.95$ ). The RMSD values were less than  $2 \text{ MJ m}^{-2} \text{ d}^{-1}$  for 12 methods at Clay Center and for 14 methods at Davis. The slope of the best-fit line ranged from 0.60 to 1.19 at Davis and from 0.76 to 1.37 at Clay Center. The RMSD ranged from 0.45 to  $7.16 \text{ MJ m}^{-2} \text{ d}^{-1}$  at Davis and from 0.44 to  $5.68 \text{ MJ m}^{-2} \text{ d}^{-1}$  at Clay Center. The performance of some of the methods showed

Table 3. Statistical analyses (two-tailed t-test for two-sample for means) between the  $R_n$ ,  $ET_o$ , and  $ET_r$  values calculated using two surface albedo values ( $\alpha = 0.23$  vs.  $\alpha = 0.19$  for each pair variable). Analyses were done for 2005 season using the data from 1 June to 30 September ( $n = 122$  for each case).

Variable	Mean		Variance		t-test (two-tail)		p-Value (p<0.05) <sup>[a]</sup>
	$\alpha = 0.23$	$\alpha = 0.19$	$\alpha = 0.23$	$\alpha = 0.19$	$t_{\text{computed}}$	$t_{\text{critical}}$	
Net radiation ( $R_n$ )	12.7	13.5	11.97	13.57	-1.884	0.0596	0.0596 <sup>NS</sup>
Grass-reference $ET$ ( $ET_o$ )	4.86	5.07	2.23	2.38	-1.075	1.9599	0.2821 <sup>NS</sup>
Alfalfa-reference $ET$ ( $ET_r$ )	6.10	6.30	4.39	4.55	-0.756	1.9599	0.4490 <sup>NS</sup>

[a] NS = not significant at 5% significance level.

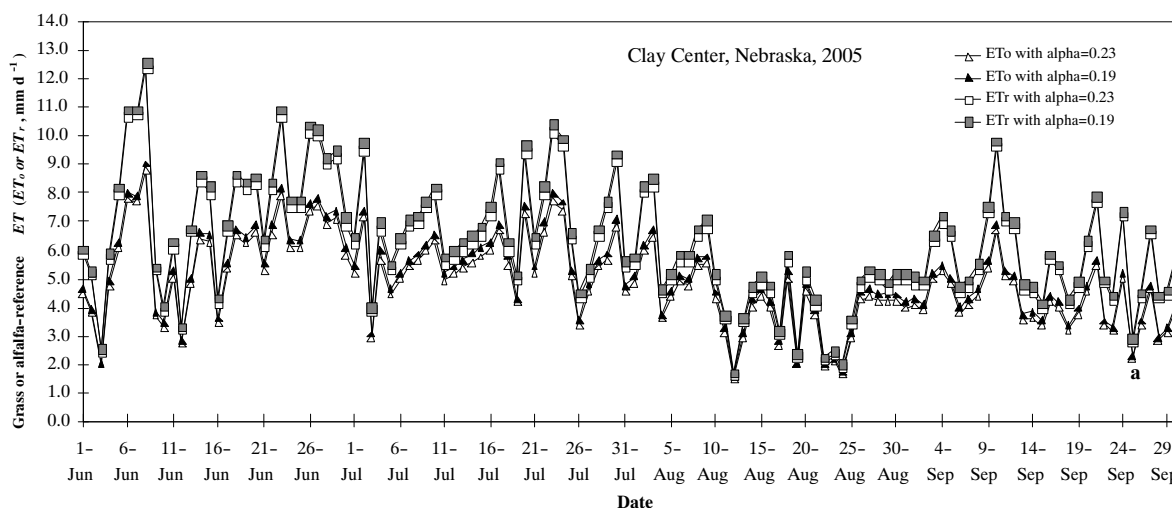
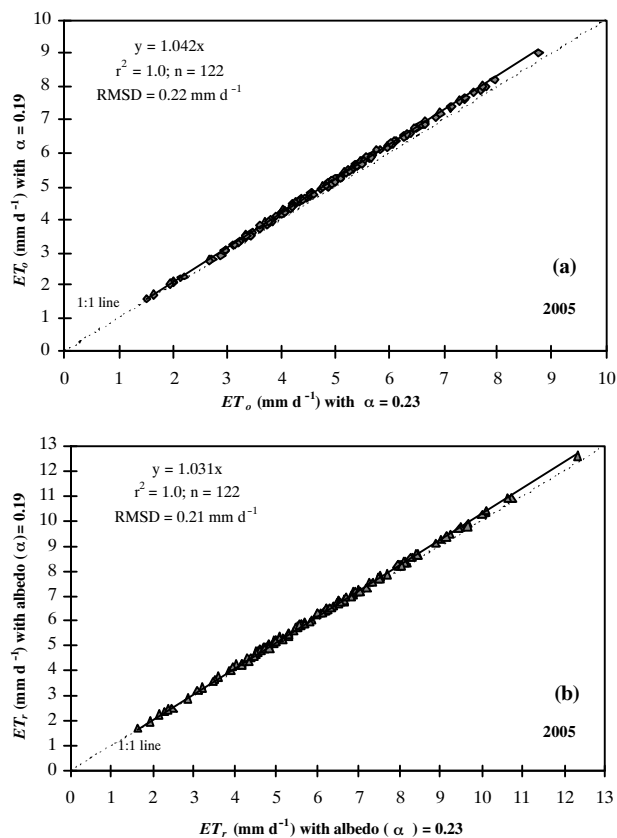


Figure 4. Grass- and alfalfa-reference evapotranspiration ( $ET_o$  and  $ET_r$ ) calculated using surface albedo ( $\alpha$ ) of 0.23 versus 0.19 for 2005 growing season.

considerable variations between the two locations. For example, method 8 had a greater  $r^2$  and lesser RMSD (0.78 and 3.72 MJ m<sup>-2</sup> d<sup>-1</sup>, respectively) at Davis than at Clay Center ( $r^2 = 0.57$  and RMSD = 5.28 MJ m<sup>-2</sup> d<sup>-1</sup>), whereas method 17 performed better at Clay Center with  $r^2$  of 0.78 and RMSD of 3.64 MJ m<sup>-2</sup> d<sup>-1</sup> than at Davis with  $r^2$  of 0.85 but a much greater RMSD (7.16 MJ m<sup>-2</sup> d<sup>-1</sup>). Methods 1, 6, 11, and 18 had the greatest  $r^2$  values at Davis. Methods 1, 3, 11, and 18 had the greatest  $r^2$  at Clay Center. In general,  $r^2$  values were greater for Davis (semi-arid) than for Clay Center (sub-humid). The differences in the performance of the methods in two climates might be due to the differences in the influence of the climatic pattern on  $R_{nl}$ . Davis has less fluctuations in  $u_2$ ,  $T$ ,  $RH$ , rainfall, and cloud cover during the summer months, whereas the fluctuations in these variables are very high in the summer months at Clay Center, contributing to differences in performance for some methods.

Methods 1, 3, 4, 6, 10, 11, 13, and 18 were very similar and were remarkably close to the ASCE-EWRI  $R_n$  calculations in both locations. For example, method 1 had an  $r^2$  of 0.99 at both locations and RMSD of 0.44 MJ m<sup>-2</sup> d<sup>-1</sup> at Clay Center and 0.84 MJ m<sup>-2</sup> d<sup>-1</sup> at Davis. Method 1 overestimated ASCE-EWRI  $R_n$  only by 5% at Davis, whereas the slope of the regression line was 1.0 at Clay Center. Method 18 had an  $r^2$  of 0.99 in both locations and underestimated ASCE-EWRI  $R_n$  by only 1%. It had RMSD of 0.47 and 0.45 MJ m<sup>-2</sup> d<sup>-1</sup> at Clay Center and Davis, respectively. The best performing equations (eqs. 6, 13, and 18) use equations 18, 5, and 19, respectively, to calculate  $R_{so}$ . They use equation 15 to calculate  $\epsilon$ , and use constants  $a_1$  and  $b_1$  ( $a_1 = 0.35$ ;  $b_1 = -0.14$ ). Good performance of these methods in both locations that have different climatic patterns indicates the transferability of constants 0.35 and -0.14 between the locations and robustness of the procedures although they differed slightly in performance between the locations. This is most likely due to using the same constants in two different climatic conditions. Equations 1, 3, 4, 10, and 11 use different equations to calculate  $R_{so}$ , but they all use equation 17 to calculate  $\epsilon$  as a function of mean air temperature, as developed by Idso et al. (1969) and Idso and Jackson (1969). By using equation 17 to calculate  $\epsilon$ , all five equations had lower RMSD at Clay Center than Davis. The structure of methods 6, 13, and 18 are very similar to the ASCE-EWRI  $R_n$  procedures. They differ in estimating  $R_{so}$  and use different values for constants  $a$ ,  $a_1$ ,  $b$ , and  $b_1$ . The ASCE-EWRI uses  $a = 1.35$ ,  $b = -0.35$ ,  $a_1 = 0.34$ , and  $b_1 = -0.14$ . Since a single



**Figure 5. Relationship between (a) grass-reference evapotranspiration ( $ET_0$ ) and (b) alfalfa-reference evapotranspiration ( $ET_r$ ) as calculated using Penman-Monteith equation. Two sets of  $ET_0$  and  $ET_r$  values were calculated using net radiation ( $R_n$ ) and surface albedo ( $\alpha$ ) of 0.23 and 0.19 to quantify the impact of two  $\alpha$  values on  $ET_0$  and  $ET_r$ .**

temperature measurement at the canopy height is used, the term  $(0.34 - 0.14\sqrt{e_a})$  in equation 3 of the ASCE-EWRI  $R_n$  procedure should be similar to  $\epsilon$ , representing the difference between the  $\epsilon$  for the field and the effective  $\epsilon$  for the surrounding atmosphere. The equation developed by Idso et al. (1969) and Idso and Jackson (1969) to estimate  $\epsilon$  differs from the one used in the ASCE-EWRI  $R_n$  procedure in that it is more generalized, uses variable  $\epsilon$ , and is based on a single canopy height mean air temperature, whereas the ASCE-EWRI procedure is based on the assumption that the ground

**Table 4. Statistical analyses (autocorrelation, AC) between method-estimated net radiation ( $R_n$ ) and ASCE-EWRI approach estimated  $R_n$  for Clay Center, Nebraska (1983-2004) and Davis, California (1990-2004). The autocorrelation analyses on residuals were conducted at the 5% significance level with null hypothesis that there is no first-order autocorrelation ( $n = 8,036$  for Clay Center and  $n = 5,479$  for Davis). The regress r-squared values (RRS coeff.) between the ASCE-EWRI  $R_n$  and method-estimated  $R_n$  are also included.**

$R_n$ Method	Clay Center, Nebraska					Davis, California				
	RRS Coeff.	DW Statistics	p-Value (p<0.05)	Intercept	Slope	RRS Coeff.	DW Statistics	p-Value (p<0.05)	Intercept	Slope
4	0.9846	1.8531	<0.05	0.7514	0.9417	0.9834	1.9399	<0.05	1.0655	0.8650
7	0.8706	1.5116	<0.05	3.9339	0.7445	0.9210	1.5289	<0.05	3.7566	0.6958
8	0.6919	1.6467	<0.05	4.9007	0.8572	0.9010	1.3710	<0.05	4.2775	0.7814
9	0.9123	1.5344	<0.05	3.9199	0.7616	0.9445	1.6155	<0.05	3.4632	0.7658
10	0.9846	1.8894	<0.05	0.7582	0.9758	0.9831	1.9479	<0.05	1.1418	0.8934
13	0.9969	1.9410	<0.05	0.9632	0.9652	--	--	--	--	--
15	0.8680	1.4501	<0.05	-0.0260	0.9673	0.9196	1.4799	<0.05	-0.3509	0.9279
16	--	--	--	--	--	0.9601	1.9419	<0.05	-0.7417	1.0043
18	0.9977	1.9300	<0.05	0.6958	0.9312	--	--	--	--	--

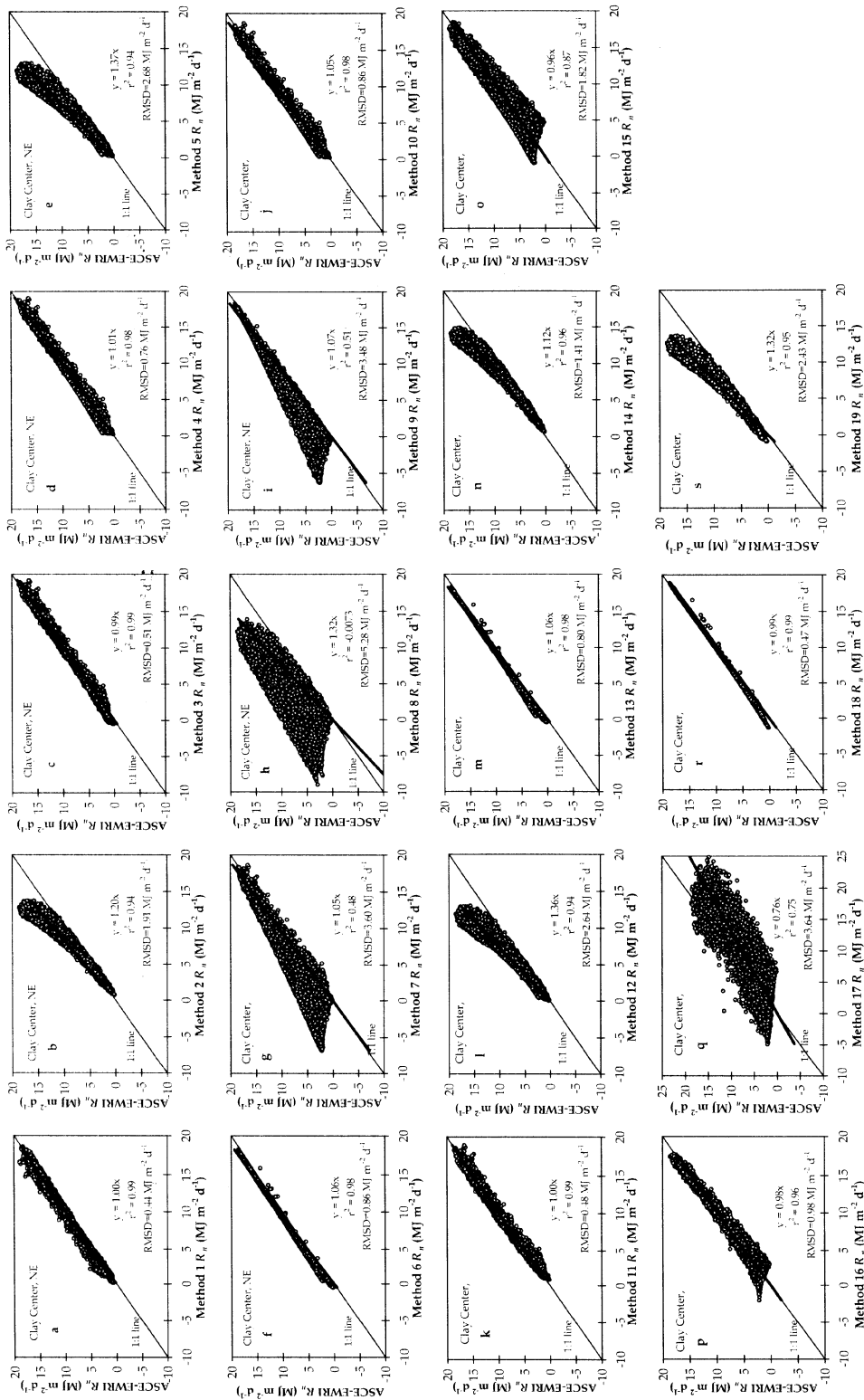


Figure 6. Relationship between the estimated daily  $R_n$  values using 19 methods and the ASCE-EWRI  $R_n$  values for calendar year for Clay Center, Nebraska ( $n = 8,036$  for each case).

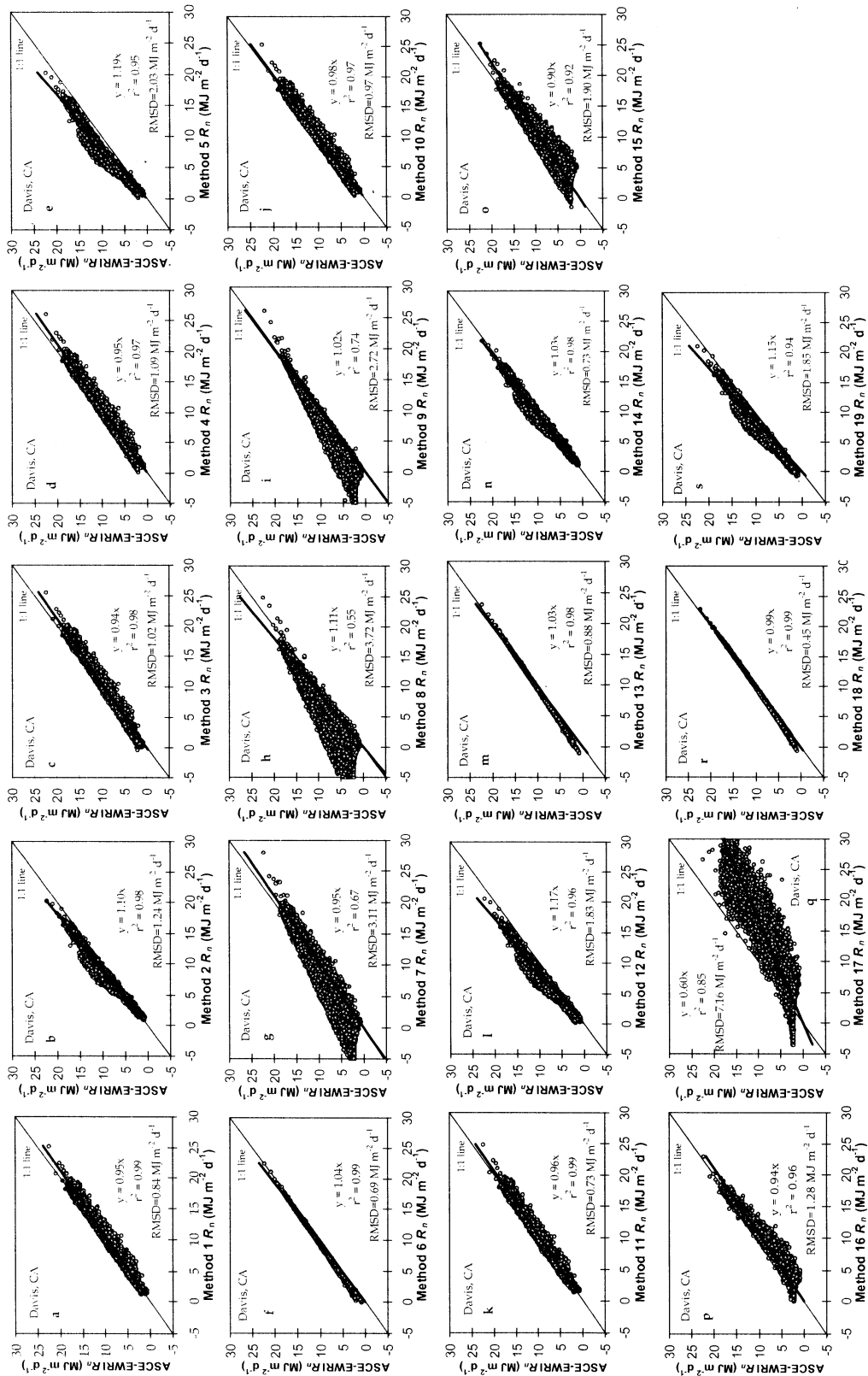


Figure 7. Relationship between the estimated daily  $R_n$  values using 19 methods and the ASCE-EWRI  $R_n$  values for the calendar year for Davis, California ( $n = 5,479$  for each case).

and vegetation surface have a constant  $\epsilon$  of 0.98. The ASCE-EWRI  $R_n$  procedure accounts for  $e_a$ , however.

The assumption  $\epsilon = 0.98$  is valid for a mean air temperature of 21.1°C based on equation 17. However, the

mean air temperature can fluctuate plus or minus several degrees from 21.1°C during a growing season. As figure 8 shows,  $\epsilon$  is a strong function of air temperature and  $\epsilon$  can deviate from 0.98 substantially during the season as a

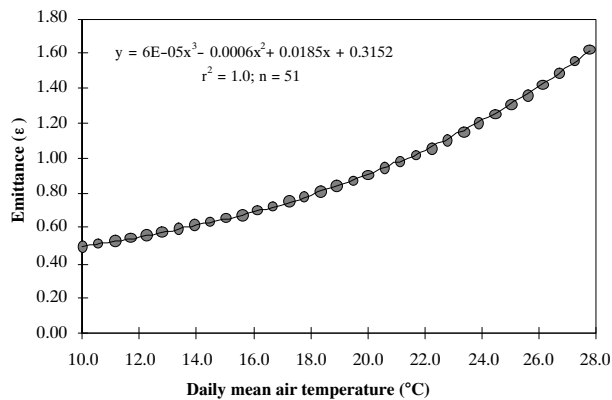


Figure 8. Relationship between emittance and mean air temperature.

function of changes in air temperature. While a constant  $\epsilon = 0.98$  is the case for a green vegetation surface for the majority of the growing season, a variable  $\epsilon$  as a function of air temperature should provide more realistic  $R_n$  values, because it will account for the impact of sudden temperature fluctuations on  $\epsilon$  and  $R_n$ . Accounting for abrupt changes in air temperature is especially important in locations such as Clay Center, Nebraska, where fluctuations in weather variables are large. The slight differences in estimating  $R_{so}$ ,  $\epsilon$ , and other parameters resulted in slight differences in performance between equations 6, 13, and 18 and the ASCE-EWRI  $R_n$  at both study locations (figs. 6f, 1m, 1r, 2f, 2m, and 2r).

In figure 6, methods 7, 8, 9, and 15, and to a lesser extent method 16, exhibited a triangular-shaped distribution of the data (funnel effect) with larger scatter of data points in the lower range of  $R_n$  and narrower scatter with increasing  $R_n$ . This wide range of the  $R_n$  data scatter is usually observed in the non-growing (dormant) season. Irmak et al. (2003) observed similar trends and suggested that the larger deviations between the ASCE-EWRI  $R_n$  and the values computed from other methods were for smaller  $R_n$  than for larger  $R_n$  and might be due to using non-calibrated values of the parameters  $0.75$  and  $2 \times 10^{-5}$  (fractions of  $R_a$  reaching the earth on overcast days) in the calculation of  $R_{so}$  (eq. 5). Although turbidity and water vapor have some influence, especially for the smaller  $R_n$  values in the winter months, this influence is usually neglected in the empirical equations when computing  $R_{so}$ . As a result, it appears that none of the equations were able to fully account for the environmental factors described in  $R_{ns}$  and  $R_{nl}$  calculations, resulting in greater deviations from the ASCE-EWRI  $R_n$  data at a smaller  $R_n$  range. In addition, because most  $R_n$  methods, including the ASCE-EWRI, were developed for estimating  $R_n$  over green vegetation, the methods appear to fail in winter since most of them did not predict any negative  $R_n$  values in winter. Negative  $R_n$  values are usually recorded in winter on relatively clear, cold, and dry days with snow and/or ice cover on the ground due to greater surface albedo and with lower sun angles and changes in effective sky emittance, which would be the case at Clay Center. In summer, methods 7, 8, 9, and 15 underestimated  $R_n$ , suggesting that the effect of cloud cover attenuation of  $R_s$  is more significant in summer than in winter.

At Clay Center, methods that used equation 17 to estimate  $\epsilon$  had the lowest RMSD values. Thus, equation 17, which

requires only mean air temperature to predict  $\epsilon$ , provided more accurate  $R_n$  estimates as compared with equation 14, which uses actual vapor pressure. In figures 6 and 7, methods 2, 5, 12, 14, and 19 exhibited a distinct structure of data distribution of near-parabolic shape. These five methods use the same equation (eq. 12) for estimating  $\epsilon$ , and the parameters  $a_1$  and  $b_1$  were computed as variable regression coefficients. The protruding data points were observed to be mainly the values for the period of March-April and early May over the 14-year period, suggesting that the performances of these methods were different in the spring. Method 16, developed by Irmak et al. (2003) for a different location (Florida), compared well with the ASCE-EWRI  $R_n$  method ( $r^2 = 0.95$  and  $0.96$  at Davis and Clay Center, respectively, and RMSD of  $1.28 \text{ MJ m}^{-2} \text{ d}^{-1}$  for Davis and  $0.96 \text{ MJ m}^{-2} \text{ d}^{-1}$  for Clay Center), given that it uses the least number of input variables ( $T_{max}$ ,  $T_{min}$ , and  $R_s$ ) and had only 6% and 2% overestimation at Davis and Clay Center, respectively.

Methods 7, 8, and 9 compared poorly to ASCE-EWRI  $R_n$  calculations, with the lowest  $r^2$  at both locations. Particularly, these methods had a cloudiness factor ( $f$ ) of 1.0, which represents completely cloudy conditions. The effect of cloud cover errors can be subjective, although these conditions are known to attenuate  $R_s$  reaching the earth surface, which explains, in part, the underestimation of ASCE-EWRI  $R_n$  by these methods. At both locations, method 17 had the highest RMSD value and overestimated ASCE-EWRI  $R_n$  by 40% at Davis and by 24% at Clay Center. Method 17 was the only method that required estimated  $R_s$ , consequently deteriorating its performance as compared with the other methods, which use measured  $R_s$ . Its performance directly and strongly depends on the accuracy of  $R_s$  estimates. Daily values of  $R_s$  for method 17 were calculated using the procedures developed by Hargreaves and Samani (1982). The comparison of the Hargreaves and Samani method (HS)-estimated daily  $R_s$  values with the measured values from 1983 to 2004 for Clay Center and from 1990 to 2004 for Davis for the calendar year are presented in figures 9a and 9b, respectively. Performance of the HS  $R_s$  method was significantly different between the two locations. While the estimated  $R_s$  values for Clay Center were within 7% (underestimation) of the measured  $R_s$  values, the HS estimates had a large standard deviation ( $7.53 \text{ MJ m}^{-2} \text{ d}^{-1}$ ), a low  $r^2$  of 0.66, and a large RMSD of  $4.31 \text{ MJ m}^{-2} \text{ d}^{-1}$  ( $n = 8,036$ ) (fig. 9a). The magnitude of RMSD and standard deviation was greater at lower  $R_s$  values ( $\leq 12 \text{ MJ m}^{-2} \text{ d}^{-1}$ ). Although the  $r^2$  was 0.90 at Davis (fig. 9b), the method's estimate was poorer at Davis, with a larger RMSD and standard deviation. The method overestimated  $R_s$  by 19%. The magnitude of overestimations increased in the higher  $R_s$  range ( $\geq 33 \text{ MJ m}^{-2} \text{ d}^{-1}$ ). The HS parameters were applied for both Clay Center and Davis without any correction or local calibration. The poor  $R_n$  estimates using method 17 suggest that the HS method parameters must be calibrated for a local region or climate, since only mean air temperature was not able to accurately account for variations in  $R_s$  at both locations.

#### COMPARISONS OF ESTIMATED DAILY $R_n$ FROM 20 METHODS WITH MEASURED $R_n$ AT CLAY CENTER

While the evaluation of the performance of different  $R_n$  methods relative to the ASCE-EWRI  $R_n$  method can provide

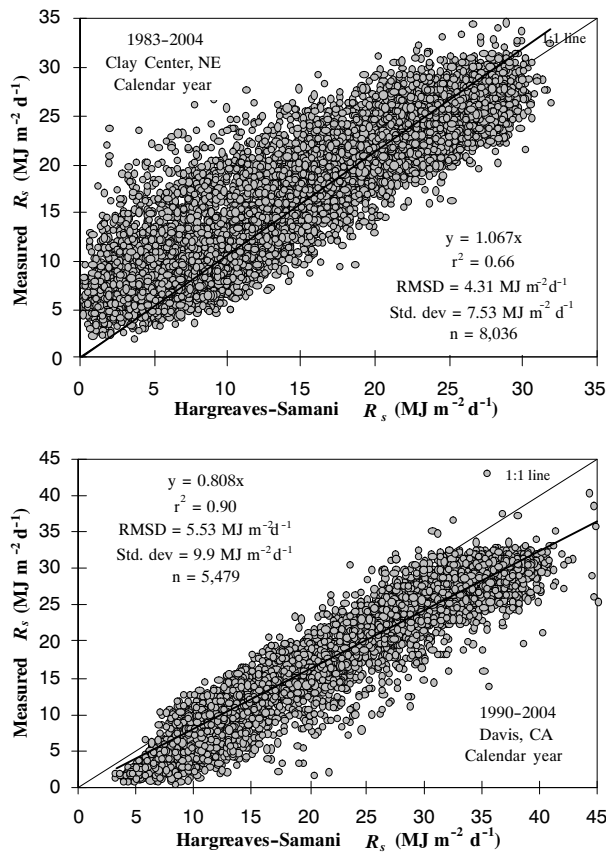


Figure 9. Estimated incoming shortwave solar radiation ( $R_s$ ) using Hargreaves and Samani (1982) method for Clay Center, Nebraska (a) and Davis, California (b).

important information regarding the dynamics and effects of different parameters and coefficients involved in  $R_n$  estimates, their performance evaluations, including the ASCE-EWRI  $R_n$  values, against measured  $R_n$  is needed. Performance evaluation of different  $R_n$  methods can provide valuable information on alternative methods to the ASCE-EWRI  $R_n$  method, depending on the availability and quality of the climate data used in  $R_n$  estimations. However, the information on the operational performance and characteristics of the ASCE-EWRI  $R_n$  method itself against measured values has not been studied sufficiently. We compared the performance of all 20  $R_n$  methods, including the ASCE-EWRI  $R_n$  values, with measured daily  $R_n$  values for a period of two growing seasons at Clay Center, and results are presented in figure 10. Figure 10 presents pooled data for the two growing seasons from 2005 and 2006. The results of statistical analyses are presented in table 5.

Overall, estimated  $R_n$  values correlated well with the measured data for most methods. Except for method 17, all methods underestimated measured  $R_n$  by a range of 6% to 23%. The  $R_n$  estimates from six methods (methods 1, 3, 11, 16, 18, and ASCE-EWRI) were not significantly different ( $p > 0.05$ ) from those measured values at the 5% significance level (table 5). The  $r^2$  values ranged from 0.64 (methods 7 and 17) to 0.95 (method 15), and the RMSD values ranged from 1.38  $\text{MJ m}^{-2} \text{d}^{-1}$  (method 18) to 4.83  $\text{MJ m}^{-2} \text{d}^{-1}$  (method 8). The ASCE-EWRI  $R_n$  values correlated well with the measured values ( $r^2 = 0.93$ ), and the estimates were within 7% of the measured  $R_n$ . Methods 18, 3, ASCE-EWRI, 16, and 4 resulted in the lowest RMSD values (1.38, 1.40, 1.44, 1.46, and 1.49  $\text{MJ m}^{-2} \text{d}^{-1}$ , respectively) and slopes closest to 1.0 ( $r^2 \geq 0.86$ ) compared to the other methods. The estimates by method 16 (eq. 28) and ASCE-EWRI were very similar in both years. Method 16 was developed and calibrated by Irmak et al. (2003) using the FAO  $R_n$  procedures (Allen et al., 1998), which are the same as the ASCE-EWRI  $R_n$  procedures

Table 5. Statistical analyses (paired t-test for two-sample for means) between measured and model-estimated  $R_n$  for 2005 and 2006 seasons (pooled data) for Clay Center, Nebraska. Analyses were done for 2005 season using measured  $R_n$  data from 1 June to 30 September at 5% significance level. The hypothesized mean difference was zero ( $n = 244$  for each case).

$R_n$ Method	Mean		Variance		t-test $t_{\text{computed}}$	p-Value ( $P_{0.05}$ ) <sup>[a]</sup>
	Estimated $R_n$	Measured $R_n$	Estimated $R_n$	Measured $R_n$		
1	11.9	12.8	12.9	16.7	-2.59	0.1150 <sup>NS</sup>
2	10.9	12.8	9.3	16.7	-5.65	0.0001*
3	12.2	12.8	13.8	16.7	-1.93	0.4390 <sup>NS</sup>
4	11.8	12.8	15.1	16.7	-3.00	0.0380*
5	9.9	12.8	10.5	16.7	-8.48	0.0001*
6	11.3	12.8	13.1	16.7	-4.48	0.0001*
7	9.8	12.8	24.8	16.7	-8.95	0.0001*
8	8.1	12.8	20.7	16.7	-13.91	0.0001*
9	9.9	12.8	21.4	16.7	-8.72	0.0001*
10	11.4	12.8	14.2	16.7	-4.17	0.0006*
11	11.9	12.8	13.3	16.7	-2.82	0.0641 <sup>NS</sup>
12	10.0	12.8	10.1	16.7	-8.23	0.0001*
13	11.4	12.8	13.2	16.7	-4.27	0.0004*
14	11.5	12.8	10.4	16.7	-3.94	0.0015*
15	11.4	12.8	14.0	16.7	-4.20	0.0005*
16	12.2	12.8	9.6	16.7	-1.73	0.5978 <sup>NS</sup>
17	15.2	12.8	14.5	16.7	6.95	0.0001*
18	12.1	12.8	13.2	16.7	-2.09	0.3365 <sup>NS</sup>
19	10.3	12.8	11.2	16.7	-7.43	0.0001*
ASCE-EWRI	12.0	12.8	12.3	16.7	-2.47	0.1534 <sup>NS</sup>

<sup>[a]</sup> NS = not significant, and\* = significant at the 5% significance level.

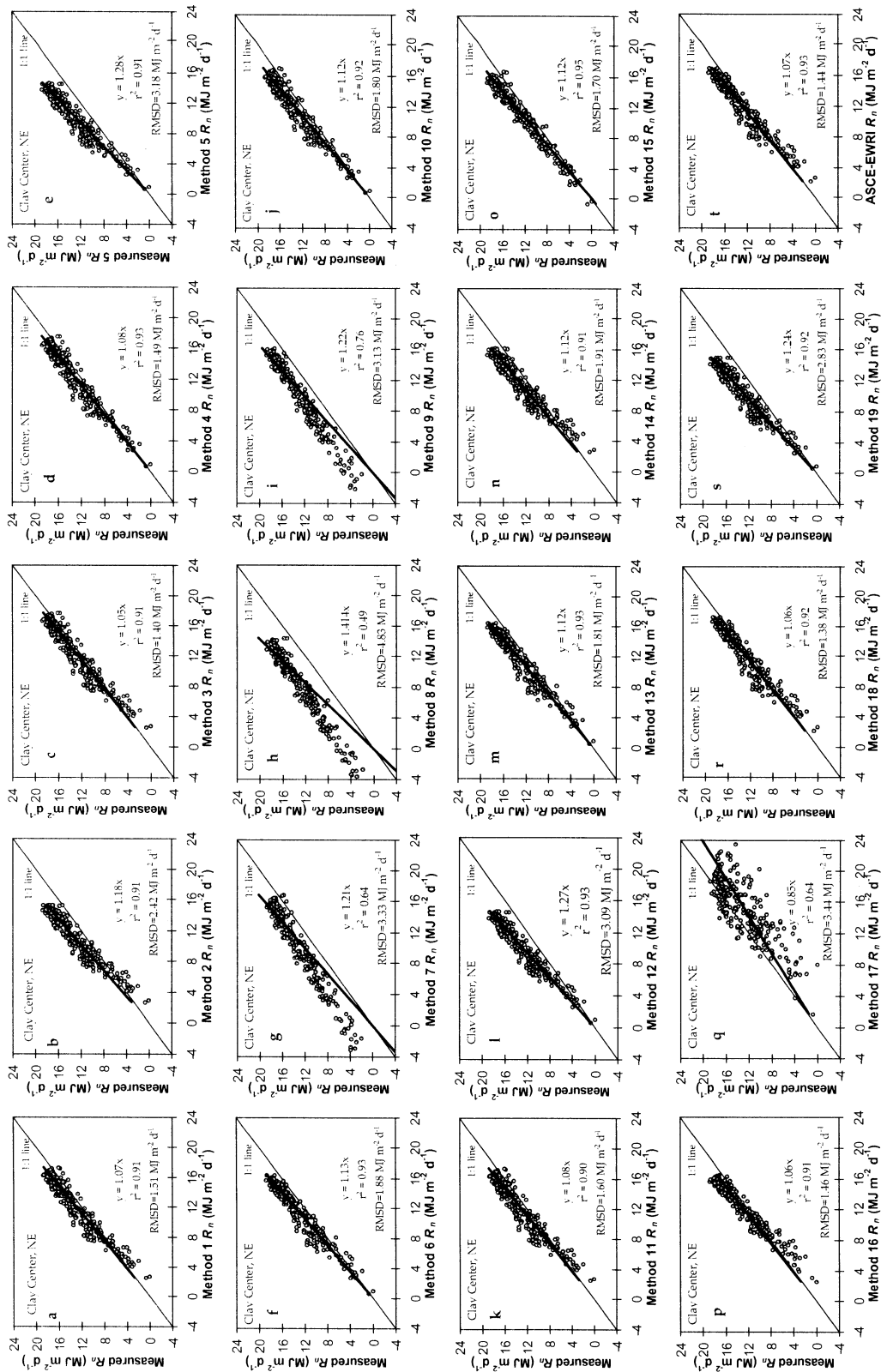


Figure 10. Regression analysis and the root mean square difference (RMSD) between the measured daily  $R_n$  and estimated  $R_n$  (19 methods and the ASCE-EWRI  $R_n$  procedure) for 2005 and 2006 growing seasons (1 June to 30 Sept.,  $n = 244$ ) (pooled data for two years) for Clay Center, Nebraska.

when applied on a daily time step for a reference humid location site. Method 16 (eq. 28) has an advantage over ASCE-EWRI in that it requires fewer inputs and can be a viable method for

estimating  $R_n$  when climate data are limited. The ASCE-EWRI method underestimated in the lower  $R_n$  range ( $\leq 12 \text{ MJ m}^{-2} \text{ d}^{-1}$ ) and overestimated for values greater than  $12 \text{ MJ m}^{-2} \text{ d}^{-1}$ .

## MEASURED VS. ESTIMATED NET LONGWAVE RADIATION ( $R_{nl}$ ) AND SENSITIVITY OF $R_n$ , $ET_o$ , AND $ET_r$ TO $R_{nl}$

A reason for the differences between estimated and measured  $R_n$  for most methods was attributed to the errors in estimation of  $R_{nl}$ . Further analyses were conducted to quantify the differences between method-estimated  $R_{nl}$  and ASCE-EWRI-estimated  $R_{nl}$ . Additional analyses were conducted to quantify the differences between the method-estimated  $R_{nl}$ , including the ASCE-EWRI  $R_{nl}$ , with the measured  $R_{nl}$  for Clay Center (table 6). With the exception of methods 5, 7, 8, 9, 12, and 19, the methods appeared to correlate reasonably with the ASCE-EWRI  $R_{nl}$ . However, the comparisons between the method-estimated  $R_{nl}$ , including the ASCE-EWRI  $R_{nl}$ , resulted in poor correlations with the measured values. The greatest  $r^2$  was obtained from methods 6, 12, and 13 as 0.57. Models 6 and 13 had the least RMSD (1.19 and 1.23 MJ m<sup>-2</sup> d<sup>-1</sup>, respectively). All methods had RMSD values greater than 1.0 MJ m<sup>-2</sup> d<sup>-1</sup>, and two methods had RMSD greater than 2.0 MJ m<sup>-2</sup> d<sup>-1</sup>. The ASCE-EWRI-estimated  $R_{nl}$  correlated poorly with the measured values ( $r^2 = 0.47$ , RMSD = 1.52 MJ m<sup>-2</sup> d<sup>-1</sup>), and it overestimated by 27%. Consequently, these errors in estimated  $R_{nl}$  are reflected in  $R_n$  estimation when comparing any methods' performance against the ASCE-EWRI  $R_n$ , and when comparing all methods, including the ASCE-EWRI  $R_n$ , with the measured values. However, although poor correlations were observed between the measured and estimated  $R_{nl}$ , most methods'  $R_n$  estimates were judged to be good. This is because, compared to net shortwave radiation,  $R_{nl}$  is a small quantity of the net radiation balance, which might explain the marginal impact of the errors in  $R_{nl}$  estimation on  $R_n$ .

**Table 6. Correlation between method-estimated  $R_{nl}$  and ASCE-EWRI  $R_{nl}$  estimates, and the method-estimated  $R_{nl}$ , including the ASCE-EWRI-estimated  $R_{nl}$  with the measured  $R_{nl}$  for maize canopy at Clay Center, Nebraska (regression equation where method-estimated  $R_{nl} = \text{slope} \times \text{method-estimated or measured } R_{nl}$ ;  $n = 244$ ). Data are for two growing seasons: from 1 June to 30 September 2005 and from 1 June to 20 September 2006.**

$R_{nl}$ Method	Method $R_{nl}$ vs. ASCE-EWRI $R_{nl}$ <sup>[a]</sup>			Method $R_{nl}$ with ASCE-EWRI $R_{nl}$ vs. measured $R_{nl}$ <sup>[b]</sup>		
	Slope	$r^2$	RMSD <sup>[c]</sup>	Slope	$r^2$	RMSD <sup>[c]</sup>
1	0.99	0.93	0.40	1.25	0.35	1.68
2	0.77	0.92	1.19	0.97	0.42	1.28
3	1.06	0.92	0.48	1.31	0.24	1.89
4	0.99	0.87	0.57	1.25	0.44	1.61
5	0.66	0.87	2.00	0.84	0.53	1.50
6	0.87	0.96	0.65	1.10	0.57	1.19
7	0.62	0.05	2.63	0.83	0.12	2.02
8	0.49	0.08	3.99	0.65	0.11	3.06
9	0.65	0.28	2.34	0.86	0.26	1.65
10	0.90	0.87	0.72	1.14	0.50	1.34
11	0.98	0.92	0.44	1.22	0.27	1.69
12	0.67	0.87	1.95	0.86	0.57	1.39
13	0.88	0.96	0.58	1.12	0.57	1.23
14	0.87	0.93	0.66	1.10	0.35	1.42
18	1.04	0.99	0.20	1.29	0.31	1.79
19	0.71	0.88	2.57	0.90	0.52	1.30
ASCE-EWRI	--	--	--	1.27	0.47	1.52

[a] Comparison between method  $R_{nl}$  and ASCE-EWRI  $R_{nl}$ .

[b] Comparison between method  $R_{nl}$  (including ASCE-EWRI  $R_{nl}$ ) and measured  $R_{nl}$ .

[c] RMSD is in units of MJ m<sup>-2</sup> d<sup>-1</sup>.

To further analyze the effect of  $R_{nl}$  on  $R_n$  and on reference  $ET$  ( $ET_o$  and  $ET_r$ ), we conducted a sensitivity analyses between these variables (fig. 11). We identified a typical summer day at Clay Center that had measured climatic variables of  $T_{max} = 32^\circ\text{C}$ ,  $T_{min} = 22^\circ\text{C}$ ,  $RH_{max} = 93\%$ ,  $RH_{min} = 40\%$ ,  $R_s = 12 \text{ MJ m}^{-2} \text{ d}^{-1}$ , and  $u_2 = 4 \text{ m s}^{-1}$ . From these variables, the ASCE-EWRI  $R_{nl}$  and  $R_n$  "base" values were calculated for the day as 0.13 and 1.41 MJ m<sup>-2</sup> d<sup>-1</sup>, respectively. All other climatic variables were kept constant while changing  $R_{nl}$ . Based on these base climate data, the daily form of the PM equation (eq. 31) was used to calculate  $ET_o$  and  $ET_r$  values as 5.23 and 7.52 mm d<sup>-1</sup>, respectively. The  $R_{nl}$  values were increased by 0.04 MJ m<sup>-2</sup> d<sup>-1</sup> increments up to 1.17 MJ m<sup>-2</sup> d<sup>-1</sup>. For every 0.04 MJ m<sup>-2</sup> d<sup>-1</sup> increase in  $R_{nl}$ , we calculated the amount of change in  $R_n$ ,  $ET_o$ , and  $ET_r$  (fig. 11). The  $R_{nl}$  effect on  $R_n$  was linear, and as expected, as  $R_{nl}$  increased, the  $R_n$  decreased. For every 0.04 MJ m<sup>-2</sup> d<sup>-1</sup> increase in  $R_{nl}$ , the  $R_n$  decreased by the same amount (0.04 MJ m<sup>-2</sup> d<sup>-1</sup>). However, the effect of  $R_{nl}$  on  $ET_o$  and  $ET_r$  was subsidiary. An increase of 0.04 MJ m<sup>-2</sup> d<sup>-1</sup> in  $R_{nl}$  resulted in an increase of 0.06 mm in  $ET_o$  and  $ET_r$ . The change in  $R_{nl}$  affected  $ET_r$  slightly more than  $ET_o$  with a slightly greater slope, -1.39 for  $ET_r$  vs. -1.43 for  $ET_o$ , but the two slopes were not significantly different ( $p > 0.05$ ). The range of increase in  $R_{nl}$  was from 0.04 to 1.17 MJ m<sup>-2</sup> d<sup>-1</sup>, and this entire increase in  $R_{nl}$  resulted in a decrease in  $ET_r$  and  $ET_o$  of 1.49 and 1.45 mm, respectively. Similar to results of the  $R_n$  impact on  $ET_o$  and  $ET_r$ , the calculation of  $R_{nl}$  over a green maize canopy rather than over grass or alfalfa did not significantly influence  $ET_o$  or  $ET_r$  calculations.

## SUMMARY AND CONCLUSIONS

We analyzed daily  $R_n$  values from 19 methods that differ in model structure and complexity. First, the estimates from all 18 methods were compared with the ASCE-EWRI  $R_n$  estimates in two climates: Clay Center, Nebraska (sub-humid) and Davis, California (semi-arid). As a second step, the  $R_n$  estimates from all 20 methods, including the ASCE-EWRI  $R_n$  values, were compared with the  $R_n$  values measured over an irrigated maize canopy at Clay Center. The majority of the models resulted in reasonable  $R_n$  estimates when compared to the ASCE-EWRI  $R_n$  values. The RMSD values between method-estimated and ASCE-EWRI-estimated  $R_n$  were lower than 2 MJ m<sup>-2</sup> d<sup>-1</sup> (0.82 mm d<sup>-1</sup>) for 12 methods at Clay Center and for 14 methods at Davis. The performance of some of the methods showed considerable differences between the two locations. In general, the  $r^2$  values were greater for the arid climate than for the sub-humid climate. Differences in model performance were attributed to differences in the influence of the general climatic patterns (more stable atmospheric conditions in summer in Davis than in Clay Center) on  $R_{nl}$ . When compared to the measured data, the ASCE-EWRI  $R_n$  values had one of the best agreements with the measured  $R_n$  data ( $r^2 = 0.93$ , RMSD = 1.44 MJ m<sup>-2</sup> d<sup>-1</sup>), and its estimates were within 7% of the measured  $R_n$ . The  $R_n$  estimates from six methods, including ASCE-EWRI, were not significantly different ( $p > 0.05$ ) from the measured  $R_n$ . Most methods underestimated measured  $R_n$  by a range of 6% to 23%. While the impact of  $R_{nl}$  on  $R_n$  is marginal, one reason for the differences between estimated and measured  $R_n$  for most

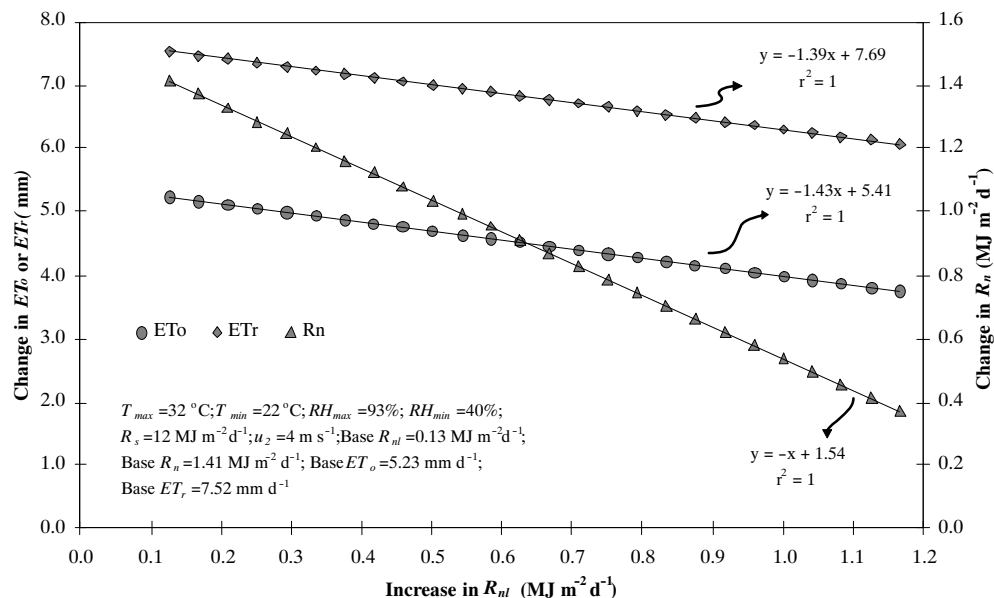


**Figure 11. Relationship between net longwave radiation ( $R_{nl}$ ), net radiation ( $R_n$ ), grass-reference evapotranspiration ( $ET_g$ ), and alfalfa-reference evapotranspiration ( $ET_a$ ) for a clear summer day, Clay Center, NE.**

methods was attributed to estimation of  $R_{nl}$ . The comparisons between the method-estimated  $R_{nl}$  with the measured values resulted in poor correlations. The ASCE-EWRI-estimated  $R_{nl}$  also correlated poorly with the measured values ( $r^2 = 0.47$ ,  $\text{RMSD} = 1.52 \text{ MJ m}^{-2} \text{ d}^{-1}$ ) with a 27% overestimation. The calculation of  $R_{nl}$  over a green maize canopy rather than over reference grass or alfalfa surfaces did not significantly influence  $ET_g$  or  $ET_a$  calculations. When the comparisons between the measured and model-estimated  $R_n$  values are considered, results suggest that the  $R_n$  data measured over green vegetation (e.g., irrigated maize canopy) can be an alternative  $R_n$  data source for  $ET$  estimations when measured  $R_n$  data are not available. Another alternative is using one of the  $R_n$  models that we analyzed when all the input variables are not available to solve the ASCE-EWRI  $R_n$  equation and when measured  $R_n$  data are not available. Our results can potentially be used to provide practical information on which method to select based on data availability for reliable estimates of daily  $R_n$  in climates similar to Clay Center and Davis.

## REFERENCES

- Allen, R. G. 1997. Self-calibrating method for estimating solar radiation from air temperature. *J. Irrig. Drain. Eng.* 2(2): 56-67.
- Allen, R. G., L. S. Pereira, D. Raes, and M. Smith. 1998. Crop evapotranspiration: Guidelines for computing crop water requirements. FAO Irrigation and Drainage Paper No. 56. Rome, Italy: United Nations FAO.
- Angstrom, A. 1924. Solar and terrestrial radiation. *Q. J. Roy. Meteorol. Soc.* 50(210): 121-125.
- ASCE-EWRI. 2005. The ASCE standardized reference evapotranspiration equation. Standardization of Reference Evapotranspiration Task Committee Final Report. R. G. Allen, I. A. Walter, R. L. Elliot, T. A. Howell, D. Itenfisu, M. E. Jensen, and R. L. Snyder, eds. Reston, Va.: ASCE Environmental and Water Resources Institute (EWRI).
- Aubinet, M., B. Chermanne, M. Vandenhaute, B. Longdoz, M. Yernaux, and E. Laitat. 2001. Long-term carbon dioxide exchange above a mixed forest in the Belgian Ardennes. *Agric. Forest Meteorol.* 108(4): 293-315.
- Bowen, I. S. 1926. The ratio of heat losses by conduction and by evaporation from any water surface. *Phys. Rev.* 27(6): 779-787.
- Brunt, D. 1932. Notes on radiation in the atmosphere. *Q. J. Roy. Meteorol. Soc.* 58(147): 389-418.
- Brutsaert, W. H. 1982. *Evaporation into Atmosphere*. Dordrecht, The Netherlands: D. Reidel Publishing.
- Deacon, E. L., and W. C. Swinbank. 1958. Comparison between momentum and vapor transfer. In *Climatology and Micrometeorology*, 38-41. UNESCO Arid Zone Research Series. Paris, France: UNESCO.
- Denmead, O. T., and I. C. McIlroy. 1970. Measurements of non-potential evaporation from wheat. *Agric. Meteorol.* 7: 285-302.
- Doorenbos, J., and W. O. Pruitt. 1977. Guidelines for prediction of crop water requirements. FAO Irrigation and Drainage Paper No. 24 (revised). Rome, Italy: United Nations FAO.
- Dyer, A. J. 1961. Measurements of evaporation and heat transfer in the lower atmosphere by an automatic eddy-correlation technique. *Q. J. Roy. Meteorol. Soc.* 87(373): 401-412.
- Finnigan, J. J., R. Clemens, Y. Malhi, R. Leuning, and H. A. Cleugh. 2003. A re-evaluation of long-term flux measurement techniques: Part I. Averaging and coordinate rotation. *Boundary-Layer Meteorol.* 107(1): 1-48.
- Fuchs, M., and C. B. Tanner. 1970. Error analysis of Bowen ratio measured by psychrometry. *Agric. Meteorol.* 7: 329-334.
- Hargreaves, G. H., and Z. A. Samani. 1982. Estimating potential evapotranspiration. *J. Irrig. Drain. Eng. ASCE* 108(3): 223-230.
- Heermann, D. F., G. J. Harrington, and K. M. Stahl. 1985. Empirical estimation of clear sky solar radiation. *J. Climate and Applied Meteorol.* 24(3): 206-214.
- Hubbard, K. G. 1992. Climatic factors that limit daily evapotranspiration in sorghum. *Climate Research* 2(1): 73-80.
- Idso, S. B., and R. D. Jackson. 1969. Thermal radiation from the atmosphere. *J. Geophys. Res.* 74(23): 5397-5403.
- Idso, S. B., R. D. Jackson, W. L. Ehler, and S. T. Mitchell. 1969. A method for determination of infrared emittance of leaves. *Ecology* 50(5): 899-902.
- Irmak, S. 2010. Nebraska Water and Energy Flux Measurement, Modeling, and Research Network (NEBFLUX). *Trans. ASABE* 53(4): 1097-1115.

- Irmak, S., and D. Mutiibwa. 2008. Dynamics of photosynthetic photon flux density and light extinction coefficient for assessing radiant energy interactions for maize canopy. *Trans. ASABE* 51(5): 1663-1673.
- Irmak, S., A. Irmak, R. G. Allen, and J. W. Jones. 2003. Solar and net radiation-based equations to estimate reference evapotranspiration in humid climates. *J. Irrig. Drain. Eng. ASCE* 129(5): 336-347.
- Irmak, S., J. O. Payero, D. L. Martin, A. Irmak, and T. A. Howell. 2006. Sensitivity analyses and sensitivity coefficients of the standardized ASCE-Penman-Monteith equation to climate variables. *J. Irrig. Drain. Eng. ASCE* 132(6): 564-578.
- Irmak, S., D. Mutiibwa, A. Irmak, T. J. Arkebauer, A. Weiss, D. L. Martin, and D. E. Eisenhauer. 2008. On the scaling up leaf stomatal resistance to canopy resistance using photosynthetic photon flux density. *Agric. Forest Meteorol.* 148(6-7): 1034-1044.
- Jensen, M. E., R. D. Burman, and R. G. Allen. 1990. *Evapotranspiration and Irrigation Water Requirements*. ASCE Manuals and Reports on Engineering Practices No. 70. Reston, Va.: ASCE.
- Monteith, J. L. 1959. The reflection of short-wave radiation by vegetation. *Q. J. Royal Meteorol. Soc.* 85(366): 386-392.
- Monteith, J. L., and M. Unsworth. 1990. *Principles of Environmental Physics*. 2nd ed. London, U.K.: Edward Arnold.
- Murray, F. W. 1967. On the computation of saturation vapor pressure. *J. Appl. Meteorol.* 6(1): 203-204.
- Oke, T. P. 1978. *Boundary Layer Climates*. New York, N.Y.: John Wiley and Sons.
- Paw, U. K. T., J. Qui, H. B. Su, T. Watanabe, and Y. Brunet. 1995. Surface energy renewal analysis: A new method to obtain scalar fluxes without velocity data. *Agric. Forest Meteorol.* 74(1-2): 119-137.
- Penman, H. L. 1956. Evaporation: An introductory survey. *Netherlands J. Agric. Sci.* 4: 9-29.
- Penman, H. L., D. E. Angus, and C. H. M. Van Bavel. 1967. Microclimatic factors affecting evaporation and transpiration. In *Irrigation of Agricultural Lands*, 483-574. R. M. Hagan, H. R. Haise, and T. W. Edminster, eds. Agronomy Monograph No. 11. Madison, Wisc.: ASA.
- Samani, Z. 2000. Estimating solar radiation and evapotranspiration using minimum climatological data. *J. Irrig. Drain. Eng.* 126(4): 265-267.
- Sellers, W. D. 1965. *Physical Climatology*. Chicago, Ill.: University of Chicago, Press.
- Snyder, R. L., and W. O. Pruitt. 1992. Evapotranspiration data management in California. *Proc. ASCE Water Forum '92*, 128-133. Reston, Va.: ASCE.
- Snyder, R. L., D. Spano, and U. K. T. Paw. 1996. Surface renewal analysis for sensible and latent heat flux density. *Boundary-Layer Meteorol.* 77(3-4): 249-266.
- Snyder, R. L., D. Spano, P. Duce, U. K. T. Paw, and M. Rivera. 2008. Surface renewal estimation of pasture evapotranspiration. *J. Irrig. Drain. Eng.* 134(6): 716-721.
- Swinbank, W. C. 1951. Measurement of vertical transfer of heat and water vapor by eddies in the lower atmosphere. *J. Meteorol.* 8(3): 135-145.
- Tanner, C. B. 1960. Energy balance approach to evapotranspiration from crops. *SSSA Proc.* 24(1): 1-9.
- Thornton, P. E., and S. W. Running. 1999. An improved algorithm for estimating incident daily solar radiation from measurements of temperature, humidity, and precipitation. *Agric. Forest Meteorol.* 93(4): 211-228.
- Webb, E. K., G. I. Pearman, and R. Leuning. 1980. Correction of flux measurements for density effects due to heat and water vapour transfer. *Q. J. Royal Meteorol. Soc.* 106(447): 85-100.
- Wright, J. L. 1982. New evapotranspiration crop coefficients. *J. Irrig. Drain. Div. ASCE* 108(IR2): 57-74.
- Wright, J. L., and M. E. Jensen. 1972. Peak water requirements of crops in southern Idaho. *J. Irrig. Drain. Div. ASCE* 96(IR1): 193-201.

## NOMENCLATURE

- $\alpha$  = albedo or canopy reflection coefficient
- $\epsilon$  = atmospheric emissivity
- $\sigma$  = Stefan-Boltzmann constant ( $4.903 \times 10^{-9}$  MJ K<sup>-4</sup> m<sup>-2</sup> d<sup>-1</sup>)
- $\omega_s$  = sunset hour angle (rad)
- $\varphi$  = latitude (rad)
- $\delta$  = solar declination angle (rad)
- $\phi$  = sun angle above the horizon (rad)
- $a$  = 1.35
- $a_1$  = 0.35
- $a_3$  = 0.61
- $a_s$  = 0.25
- $b$  = -0.34
- $b_1$  = -0.14
- $b_3$  = -1.0
- $b_s$  = -0.50
- $d_r$  = inverse relative distance from earth to sun
- $e_a$  = actual vapor pressure of the air (kPa)
- $f$  = factor to adjust for cloud cover
- $G_{sc}$  = solar constant (0.0820 MJ m<sup>-2</sup> min<sup>-1</sup>)
- $K_B$  = clearness index for direct beam radiation
- $K_D$  = clearness index for diffuse beam radiation
- $K_t$  = turbidity coefficient ( $0 < K_t \leq 1.0$ )
- $L$  = latitude
- $m$  = month of the year
- $N$  = day of the year
- $n/N$  = ratio of actual measured bright sunshine hours and maximum possible sunshine hours
- $P$  = atmospheric pressure (kPa)
- $P_o$  = mean monthly atmospheric pressure at sea level (kPa)
- PM = Penman-Monteith
- $R_a$  = extraterrestrial radiation (MJ m<sup>-2</sup> d<sup>-1</sup>)
- $R_s$  = total incoming shortwave solar radiation (MJ m<sup>-2</sup> d<sup>-1</sup>)
- $R_n$  = net radiation (MJ m<sup>-2</sup> d<sup>-1</sup>)
- $R_{so}$  = calculated clear-sky solar radiation (MJ m<sup>-2</sup> d<sup>-1</sup>)
- $R_{ns}$  = incoming net shortwave radiation (MJ m<sup>-2</sup> d<sup>-1</sup>)
- $R_{nl}$  = outgoing net longwave radiation (MJ m<sup>-2</sup> d<sup>-1</sup>)
- $RH_i$  = average relative humidity (%)
- $T_i$  = average air temperature (°C)
- $T_{max}$  = maximum air temperature
- $T_{min}$  = minimum air temperature
- $W$  = precipitable water vapor in the atmosphere (mm)
- $z$  = elevation (m)